

**SELECTED ION FLOW TUBE-MASS SPECTROMETRY
IN PLANT VOLATILE COMPOUND ANALYSIS**

By

LIANA IACHETTA

Bachelor of Science

Honours Bachelor of Science Biology

Lakehead University

Thunder Bay, Ontario, Canada

2009

**Submitted to the Faculty
of Science and Environmental Studies
Lakehead University
in partial fulfillment of
the requirements for
the Degree of
MASTER OF SCIENCE
May, 2009**

I. DECLARATION

I declare that the work presented in this thesis is original, except where otherwise acknowledged and submitted to fulfill the requirements of a Master of Science in Biology at Lakehead University, Thunder Bay, Ontario, Canada.

II. ACKNOWLEDGEMENTS

I would like to sincerely acknowledge my project advisors, Dr. Ladislav Malek, Department of Biology, Lakehead University, Dr. Brian Ross, NOSM, Lakehead University and Dr. Christine Gottardo, Department of Chemistry, Lakehead University. Dr. Malek for accepting me as a graduate student and providing me the opportunity to carry out an interesting research project, Dr. Ross for introducing me to the SIFT-MS and guiding me through all the SIFT-MS analyses and Dr. Gottardo for much appreciated advice and help with the mass spectra. Not only did my advisors provide a great deal of guidance and support, but also made these past two years an enjoyable learning experience.

I would also like to acknowledge Dr. Randolph Beaudry from Michigan State University, Department of Plant and Soil Sciences for generously providing most of the standard compounds used in this research project and Dr. Tarlok Sahota of the Thunder Bay Agricultural Research Station for providing the *Cannabis sativa* (industrial hemp) samples used in the plant analyses.

A special thank you is extended to Dr. Patrik Španěl for taking the time to review this thesis. Your input and advice is greatly appreciated.

Last but not least, I would to extend my thanks to my family, fiancé and friends for all of their support and encouragement.

III. TABLE OF CONTENTS

| | |
|--|------|
| I. DECLARATION..... | ii |
| II. ACKNOWLEDGEMENTS | iii |
| III. TABLE OF CONTENTS..... | iv |
| IV. LIST OF TABLES..... | vi |
| V. LIST OF FIGURES | vii |
| VI. LIST OF ABBREVIATIONS..... | viii |
| PART I. HEADSPACE ANALYSIS WITH A SERIES OF KNOWN MONTERPENES, MONTERPENOIDS AND ESTERS..... | 1 |
| CHAPTER 1.0. GENERAL INTRODUCTION | 1 |
| 1.1. Introduction..... | 1 |
| CHAPTER 2.0. MONOTERPENES AND MONOTERPENOIDS | 2 |
| 2.1. Abstract..... | 2 |
| 2.2. Introduction..... | 3 |
| 2.3. Experimental Section | 6 |
| 2.3.1. <i>Data Acquisition</i> | 7 |
| 2.3.2. <i>Data Handling and Display</i> | 10 |
| 2.4. Results and Discussion | 10 |
| 2.4.1. <i>Monoterpene and Monoterpenoid Reactions with H₃O⁺</i> | 10 |
| 2.4.2. <i>Monoterpene and Monoterpenoid Reactions with NO⁺</i> | 11 |
| 2.4.3. <i>Monoterpene and Monoterpenoid Reactions with O₂⁺</i> | 16 |
| 2.4.4. <i>Comparison of Results to Previous Data</i> | 16 |
| 2.5. Concluding Remarks..... | 20 |
| 2.6. Acknowledgments..... | 21 |
| CHAPTER 3.0. ESTERS | 22 |
| 3.1. Abstract..... | 22 |
| 3.2. Introduction..... | 23 |
| 3.3. Experimental Section | 27 |
| 3.3.1. <i>Data Acquisition</i> | 27 |
| 3.3.2. <i>Data Handling and Display</i> | 27 |
| 3.4. Results and Discussion | 27 |
| 3.4.1. <i>Ester Reactions with H₃O⁺</i> | 37 |
| 3.4.2. <i>Ester Reactions with NO⁺</i> | 38 |
| 3.4.3. <i>Ester Reactions with O₂⁺</i> | 39 |
| 3.5. Concluding Remarks..... | 40 |
| 3.6. Acknowledgments..... | 40 |
| PART II. SIFT-MS IDENTIFICATION OF SELECTED VOLATILE ORGANIC COMPOUNDS EMITTED FROM <i>POLYGALA SENEGA</i> , <i>VALERIANA OFFICINALIS</i> AND <i>CANNABIS SATIVA</i> | 41 |
| CHAPTER 4.0. APPLICATION OF SIFT-MS TECHNOLOGY | 41 |
| 4.1. Abstract..... | 41 |
| 4.2. Introduction..... | 42 |
| 4.2.1. <i>Selected ion flow tube-mass spectrometry</i> | 43 |
| 4.2.2. <i>Polygala senega</i> | 43 |
| 4.2.3. <i>Valeriana officinalis</i> | 44 |

| | |
|---|----|
| 4.2.4. <i>Cannabis sativa</i> | 45 |
| 4.3. Experimental Section..... | 46 |
| 4.3.1. <i>SIFT-MS Data Acquisition</i> | 47 |
| 4.3.2. <i>SIFT-MS Data Handling and Display</i> | 47 |
| 4.4. Results and Discussion | 48 |
| 4.4.1. <i>Polygala senega H₃O⁺ Reactions</i> | 49 |
| 4.4.2. <i>Polygala senega NO⁺ Reactions</i> | 63 |
| 4.4.3. <i>Valeriana officinalis H₃O⁺ and NO⁺ Reactions</i> | 64 |
| 4.4.4. <i>Cannabis sativa</i> (industrial hemp)..... | 65 |
| 4.4.4.1. <i>Cannabis sativa H₃O⁺ Reactions</i> | 66 |
| 4.4.4.2. <i>Cannabis sativa NO⁺ Reactions</i> | 67 |
| 4.5. Conclusions and Future Applications | 68 |
| 4.6. Acknowledgments..... | 71 |
| CHAPTER 5.0. REFERENCES | 72 |

IV. LIST OF TABLES

| | |
|---|-------|
| Table 1. Rate coefficients of the reactions between H_3O^+ , NO^+ and O_2^+ with a series of monoterpenes and monoterpenoids..... | 12 |
| Table 2a. Product(s) of the reactions between H_3O^+ , NO^+ and O_2^+ with a series of monoterpenes..... | 13-14 |
| Table 2b. Product(s) of the reactions between H_3O^+ , NO^+ and O_2^+ with a series of monoterpenoids..... | 15 |
| Table 3. Rate coefficients of the reactions between H_3O^+ , NO^+ and O_2^+ with a series of esters..... | 28-30 |
| Table 4. Product(s) of the reactions between H_3O^+ , NO^+ and O_2^+ with a series of esters..... | 31-36 |
| Table 5. Proposed products of the reactions between H_3O^+ and NO^+ with experimentally found compounds in <i>Polygala senega</i> | 59 |
| Table 6. Proposed products of the reactions between H_3O^+ and NO^+ with experimentally found compounds in <i>Valeriana officinalis</i> | 60 |
| Table 7. Proposed products of the reactions between H_3O^+ and NO^+ and <i>Cannabis sativa</i> leaves with experimentally found compounds in <i>Cannabis sativa</i> leaves..... | 61 |
| Table 8. Proposed products of the reactions between H_3O^+ and NO^+ and <i>Cannabis sativa</i> seeds with experimentally found compounds in <i>Cannabis sativa</i> seeds..... | 62 |

V. LIST OF FIGURES

| | |
|--|----|
| Figure 1. A diagram of the selected ion flow tube device..... | 8 |
| Figure 2. Precursor ion reaction plot..... | 9 |
| Figure 3. Analysis of <i>Polygala senega</i> ; mass spectra generated with H_3O^+ . a. m/z 1-100; b. m/z 100-200..... | 51 |
| Figure 4. Analysis of <i>Polygala senega</i> ; mass spectra generated with NO^+ . a. m/z 1-100; b. m/z 100-200..... | 52 |
| Figure 5. Analysis of <i>Valeriana officinalis</i> ; mass spectra generated with H_3O^+ . a. m/z 1- 100; b. m/z 100-200..... | 53 |
| Figure 6. Analysis of <i>Valeriana officinalis</i> ; mass spectra generated with NO^+ . a. m/z 1- 100; b. m/z 100-200..... | 54 |
| Figure 7. Analysis of <i>Cannabis sativa</i> leaves; mass spectra generated with H_3O^+ . a. m/z 1-100; b. m/z 100- 200..... | 55 |
| Figure 8. Analysis of <i>Cannabis sativa</i> leaves; mass spectra generated with NO^+ . a. m/z 1-100; b. m/z 100-200..... | 56 |
| Figure 9. Analysis of <i>Cannabis sativa</i> seeds; mass spectra generated with H_3O^+ . a. m/z 1-100; b. m/z 100-200..... | 57 |
| Figure 10. Analysis of <i>Cannabis sativa</i> seeds; mass spectra generated with NO^+ . a. m/z 1-100; b. m/z 100-200..... | 58 |

VI. LIST OF ABBREVIATIONS

| | |
|----------|---|
| (+) | Clockwise rotation (optical activity) |
| DL- | Dextarotary/Levorotary rotation (structure configuration) |
| (E) | Entgene (<i>trans</i> isomerism) |
| (1S) | Sinister rotation (structure configuration) |
| α | Polarizability |
| μ | Permanent dipole moment |
| AIDS | Acquired Immune Deficiency Syndrome |
| API-MS | Atmospheric pressure ionization- mass spectrometer |
| cps | Counts per second |
| D | Debye |
| FDA | Food and Drug Administration |
| GC | Gas chromatography |
| GC-MS | Gas chromatography-mass spectrometry |
| GC-O | Gas chromatography-olfactometry |
| HTS | High throughput screening |
| k | Rate coefficient |
| kc | Collisional rate coefficient |
| MS | Mass spectrometry |
| m | Molecular weight |
| mL | Millilitre |
| muview | MUI File Viewer |
| msview | Mass Spectrometry Review |
| NCE | New chemical entities |
| SIFT | Selected ion flow tube |
| SIFT-MS | Selected ion flow tube-mass spectrometry |
| THC | Tetrahydrocannabinol |
| torr | Non-SI unit of pressure (SI=International System of Unit) |
| u | atomic units |
| VOC | Volatile organic compound |

PART I. HEADSPACE ANALYSIS WITH A SERIES OF KNOWN MONOTERPENES, MONOTERPENOIDS AND ESTERS

CHAPTER 1.0. GENERAL INTRODUCTION

1.1. Introduction

Natural products are chemical compounds derived from wild and domesticated plants and may have commercial application or biological activity. Plants synthesize and emit biologically active compounds as volatiles that interact with human receptors to provide sensation of odour and flavour [51, 72]. In this thesis, I am concentrating on volatile organic compounds (VOCs) as food flavours, cosmetic products and medicinals. I analyse several known volatile compounds from plants and confirm the detection of such compounds by SIFT-MS, and extend this work to known compounds from three selected plants.

The current study is divided into two parts. In part 1, typical odour and flavour compounds are analyzed using the SIFT-MS to confirm and expand on the existing data library of spectra of various compounds. Compounds of particular interest are monoterpenes and monoterpeneoids, as well as esters. In part 2, the usefulness of SIFT-MS in natural product research is examined, by correlating the results from standard compound analyses with actual mass spectra from plant material.

CHAPTER 2.0. MONOTERPENES AND MONOTERPENOIDS

2.1. Abstract

Four monoterpenes and two monoterpeneoids, (+)- and DL- limonene, (1S)-(3) carene, terpinolene, cineol and rose oxide, respectively, were studied using selected ion flow tube-mass spectrometry. Specifically, the reactions of H_3O^+ , NO^+ and O_2^+ were used to examine these compounds. The H_3O^+ reactions resulted in the generation of two major product ions, $\text{C}_{10}\text{H}_{16}\cdot\text{H}^+$ and C_6H_9^+ , for the monoterpenes and $\text{C}_{10}\text{H}_{18}\text{O}\cdot\text{H}^+$ for monoterpeneoids with the addition of fragment ions $\text{C}_{10}\text{H}_{17}^+$ and $\text{C}_6\text{H}_{11}\text{O}^+$ for rose oxide. Charge transfer, $\text{C}_{10}\text{H}_{16}^+$, was the main product ion for the NO^+ reaction with the monoterpenes, although, fragment ions were also detected, particularly, $\text{C}_9\text{H}_{13}^+$ and C_7H_9^+ . Similar to the monoterpenes, the parent monoterpeneoid, $\text{C}_{10}\text{H}_{18}\text{O}^+$, was produced for both cineole and rose oxide with the addition of a fragment $\text{C}_9\text{H}_{15}\text{O}^+$ for rose oxide. Based on the minority product ions and/or adduct ions produced in the H_3O^+ and NO^+ reactions, the identification of the parent compound can be made. O_2^+ reactions often result in greater fragmentation. However, I have shown that for some molecules, few fragment ions are produced and thus may provide additional information leading to the identification of the parent compound as well. SIFT-MS provides a means of detection and identification of these compounds, without destroying the sample of interest. In the case of monoterpenes and monoterpeneoids, the SIFT can be utilized to estimate the total terpene content present in a sample [100].

2.2. Introduction

I set out to investigate the applicability of selected ion flow tube-mass spectrometry (SIFT-MS) to plant derived aromatic compounds, particularly in respect to its potential in high throughput screening (HTS) for bioactive compounds. Odourants are volatile chemicals that are inhaled in the nasal olfactory epithelium located in the nasal cavity, while flavour is the blend of odour and taste [12, 72]. Humans have been interested in the unique and pleasantly fragrant odours produced by plants for a long time and have used plants to flavour and season food stuffs, as well as develop primitive cosmetics [8, 72]. This interest led to the use of plants as more than a means of nutrition, but as a way to improve bodily scent by use of simple cosmetics, and possibly to provide health-restoring medicinal action. This use of plants as remedial agents dates back to the time of the Sumerian and Akkadian civilizations, third millennium B. C. [8, 14]. It was discovered that the active compounds in the plant material could be separated by gentle heating resulting in an oil-aqueous mixture known as essential oils [8]. Essential oils from plants contribute to the powerful aromatic odours which are desirable in food and cosmetic preparations [72]. The production and use of essential oils became a major element in medicinal practices during the 16th century [8]. The association of pleasant aromas with the sense of well being resulted in the modern practice of aromatherapy. However, scientific evidence for a link between essential oil sensory detection and restoring health is still lacking [54]. Chemical analyses of these oils did not occur until the 19th century, when single compounds responsible for a specific odour were beginning to be isolated [8, 70, 72]. It was found that the volatile fractions were to a large extent composed of hydrocarbons of the formula $C_{10}H_{16}$, or monoterpenes [8, 70].

Terpenes and their oxygenated derivatives, terpenoids, are the most diverse families of natural products possessing functional groups such as alcohols, hydrocarbons and ketones, for example, with over 40,000 known structures [8, 36, 72]. They are present in, and emitted from many plant species, and their various organs such as leaves, roots, flowers and fruits [100, 103]. Some terpenes produced from plants are of commercial and medicinal importance [70, 72]. Many are shown to possess pleasant odours and are used as flavouring agents and perfumes, while others possess bioactive properties and are used as antimicrobials, insecticides and medicinal preparations [70, 72]. For example, menthol is applied topically to soothe skin irritation [11], limonene has chemo-preventive and therapeutic properties in rodent models [34] and camphor acts as an insect repellent [43]. Discovery of additional biological functions of terpenoids requires the development of new, rapid analytical methods. The complex structure of terpenes in natural mixtures leads to the need for separation and subsequent identification of individual compounds [8]. HTS is a method used to detect biological activity from various sources [5]. The main function of HTS is to efficiently accelerate the drug discovery process by screening large libraries containing hundreds of thousands of chemical compounds for potentially active compounds [6, 7, 107]. Screening molecular signature computer databases against similar chemical signals exhibited by unknown compounds is a suitable approach for compound identification [1, 14]. We chose to start establishing a database of SIFT-MS signatures of specific compounds, with the intent that this may ultimately aid in HTS of plant bio-products and possibly drugs.

Drug discovery requires the union of chemistry, pharmacology and clinical sciences [13, 23]. In some countries, natural products remain a highly sought-after

source of medicine. In China, for example, 7, 295 plant species are used as therapeutics [14]. Hundreds of compounds can be potentially present in plant material. To detect and identify all of these compounds is an expensive, time-consuming and labour intensive task. The difficulties associated with creating a natural product data library have eased with the development of new analytical devices [14], such as SIFT-MS introduced below.

The selected ion flow tube-mass spectrometer may have the capacity to analyse plant volatiles without the need for prior separation. Developed in the 1970s, SIFT-MS is one of the most reliable techniques available for the study of kinetics and ionic reactions [4, 90]. It is a successful chemical ionization method used to (1) detect and identify volatile compounds of commercial or medicinal value, as well as (2) expand the knowledge of constituents in a sample/product of interest. SIFT technology is now a standardized method for trace gas analysis for the rapid detection and quantification of VOCs [49, 75]. For example, SIFT-MS has been utilized for various headspace studies, such as volatile food flavours [89], bacterial emissions [17], medical breath analysis [62] and pollution [77]. H_3O^+ , NO^+ and O_2^+ are the reactive precursor ions used to react with unknown compounds to produce identifiable secondary ions [76, 81]. This work continues the task set out by Španěl and Smith [87] to utilize the potential analytical advantages of SIFT-MS to rapidly analyze mass spectra and reaction kinetics of known compounds to keep expanding the library of SIFT-MS data. These standards will be subsequently correlated with real time spectra of actual plant material. The current study focuses on the results of the reactions between H_3O^+ , NO^+ and O_2^+ with four monoterpenes and two monoterpenoids (Table 1).

2.3. Experimental Section

I adopted SIFT-MS methodology developed by Adams and Smith [3]. A brief summary of SIFT-MS theory follows, based on a diagram in figure 1 and previous published work [75, 78, 83].

Fast flow tube techniques are an ideal method to analyze and examine ion neutral reactions under thermal conditions. The production of primary ions (H_3O^+ , NO^+ and O_2^+) takes place in a microwave resonator. H_3O^+ , NO^+ and O_2^+ then pass through the injection quadrupole mass filter which filters through the ions which have been pre-selected. The selected ion(s) travel through the ion injection orifice into the flow tube and are carried down the tube by helium gas. The ions react with the trace gas containing the molecules of interest and produce secondary product ions and/or fragment ions. The secondary product ions and/or fragment ions pass through the ion sampling orifice where a detection quadrupole mass spectrometer filters through any ions which fall within a pre-selected mass-to-charge ratio range. These ions are detected and counted by a channeltron ion detector and the resulting information is visualized as mass spectra (Fig. 1).

Rate coefficient and ion product distribution of a reaction must be known [86]. The rate coefficient quantifies the speed of a chemical reaction. Some standard compounds may produce product ions with the same molecular weight. Rate coefficient data can be used to differentiate these types of standard compounds because the speed, at which the resulting ions are formed, will most likely differ. Ion product distribution is determined by injecting the reaction ion species, determining the product ion as a function of the flow rate of the reactant gas and extrapolating the flow rate curves to zero [75, 86]. Knowledge of the flow rate is required to determine the rate coefficient [86].

The flow rate was measured using a gas flow meter (Scienceware (Riteflow), Fisher Scientific, Ottawa, Ontario, Canada). If exothermic proton transfer reactions are comparable to the collisional rate, it can be assumed that k is equal to the collisional rate coefficient k_c [9, 86]. The Su and Chesnavich equation is used to calculate k_c [92]. Dipole moment and polarizability of a reaction are required to compute k_c [84]. These assumptions cannot be made for NO^+ and O_2^+ , therefore, k must be determined experimentally [86]. I used solutions of unknown concentration of the monoterpene and monoterpenoid standard compounds for rate experiments. H_3O^+ , NO^+ and O_2^+ , were introduced into the SIFT and precursor ion reaction plots as a function of flow rate of the reactant gas were obtained [86]. Relative k values for NO^+ and O_2^+ were deduced from the slopes of the precursor ion reaction plots (Fig. 2) [86].

2.3.1. Data Acquisition

SIFT-MS analysis was performed using a Profile 3 SIFT-MS spectrometer (Instrument Science, UK). I placed open vials with standard solution of monoterpene under the SIFT intake nozzle, choosing multi-ion monitoring mode cycling of all three precursor ions, H_3O^+ , NO^+ and O_2^+ , for analysis. Each sample was analyzed at least twice, by performing 1 scan of 60 second duration. I also analyzed laboratory air, to allow me to subtract this background from actual sample mass spectra. Mass spectra produced are visual representations of the secondary product ions created by SIFT-MS analysis. Standard solution spectra illustrate the product ions generated from the chemical ionization reactions that occur between the chosen precursor ion(s) and molecules emitted from the sample.

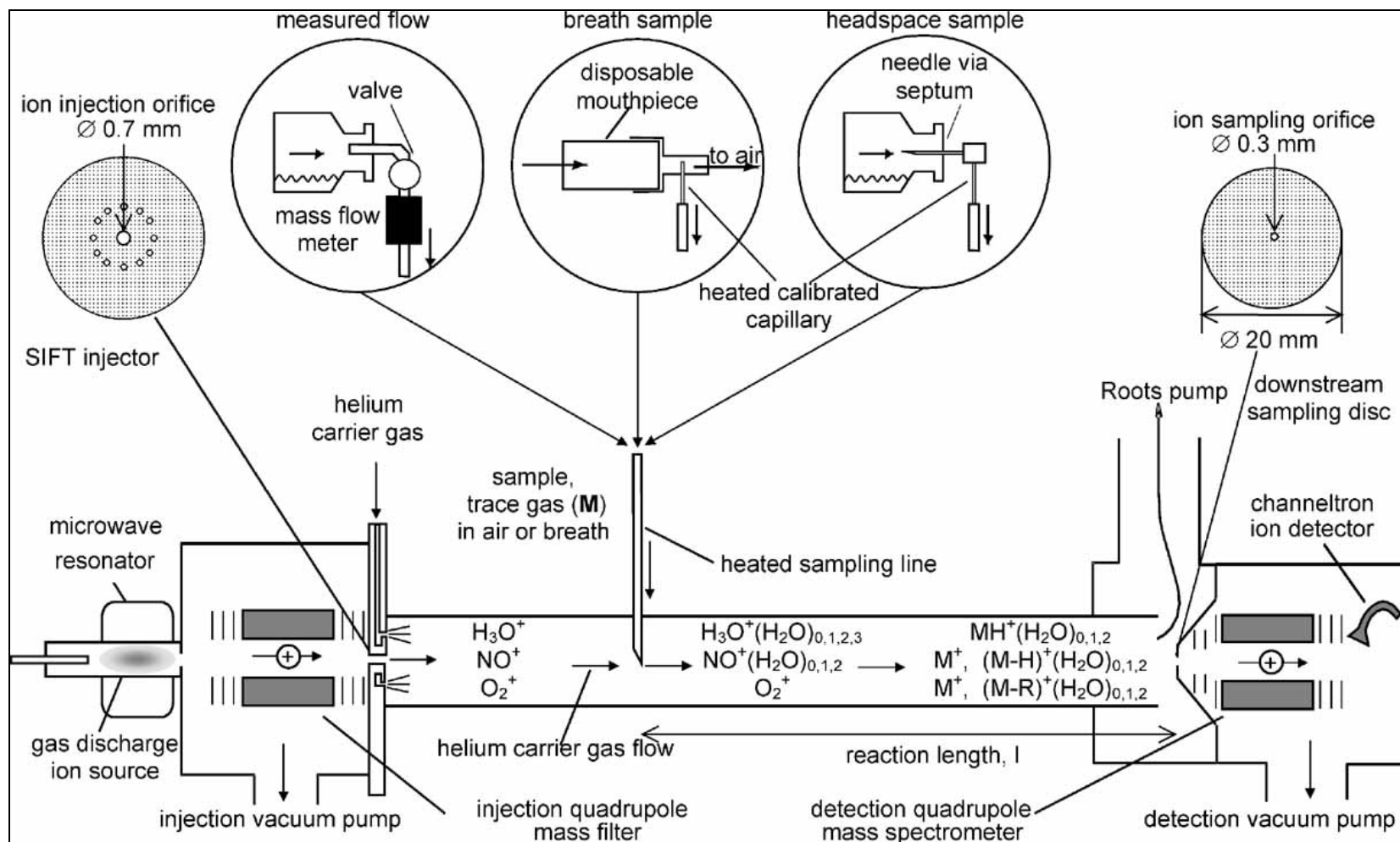


Figure 1. A diagram of the selected ion flow tube-mass spectrometry (SIFT-MS) device [77]. Precursor ions enter the flow tube (upstream) and react with sample compounds to produce product ions (downstream). Various methods of sample introduction are illustrated in the circles.

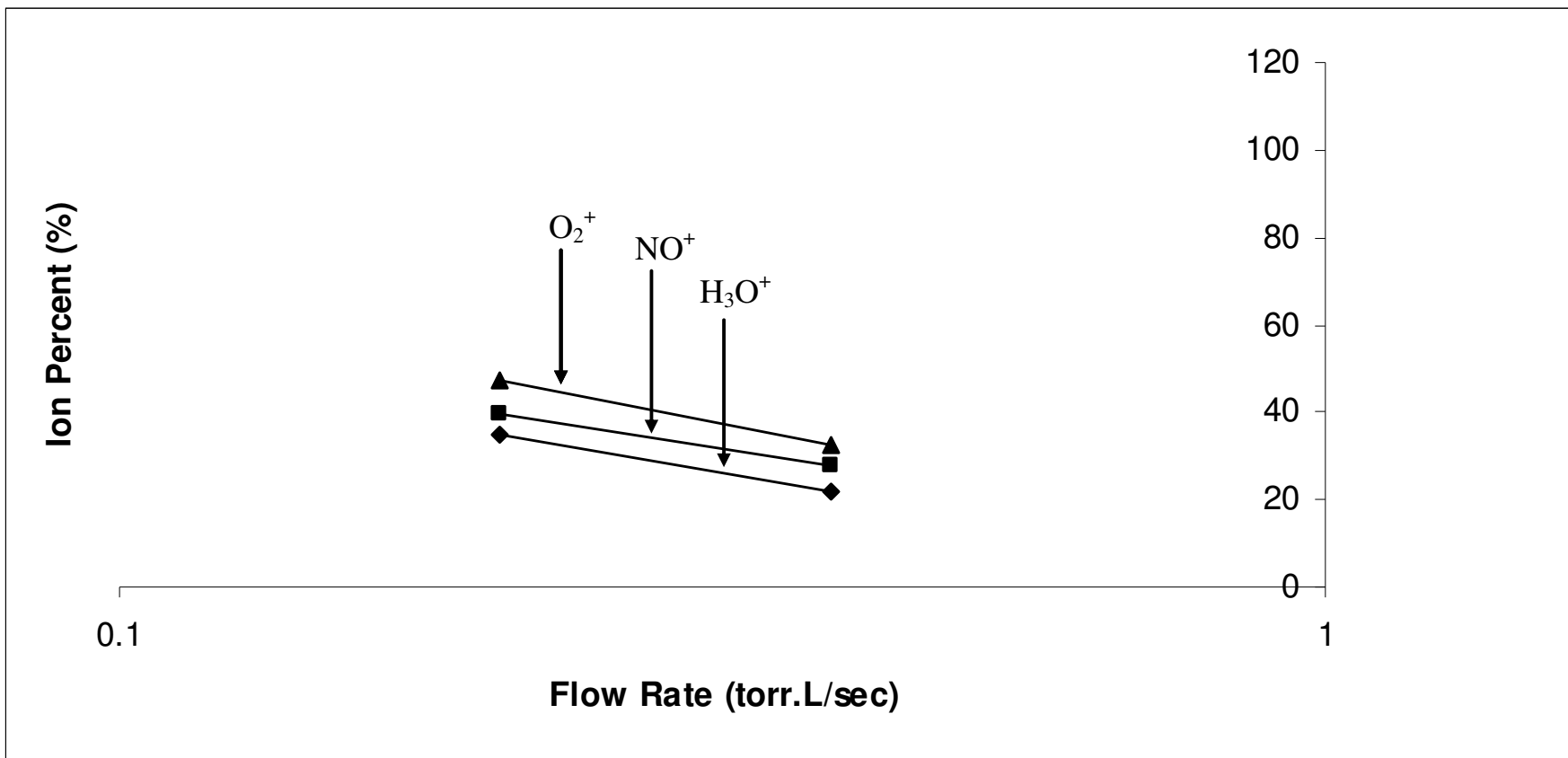


Figure 2. Precursor ion reaction plot. The above plot is an example using cineole.

2.3.2. *Data Handling and Display*

Using the Mass Spectrometry Review (msview) software that accompanies the SIFT-MS instrument, I exported spectra from the SIFT-MS data system into Microsoft Excel, to complete calculations. An average of the product ions produced from each standard solution was calculated. The averaged values were then visualized as spectra for each sample. Major peaks represent the most abundant product ions produced. These product ions were then confirmed to be in the sample using MUI File Viewer (muiview). Confirmed product ions were used to finalize the identification of the VOCs emitted from the standard solutions.

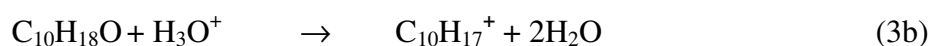
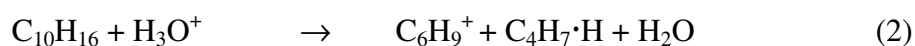
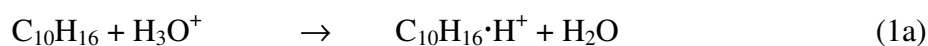
2.4. Results and Discussion

Calculated k_c for the H_3O^+ proton transfer reactions and the experimentally determined k with k_c for the NO^+ and O_2^+ reactions with the monoterpenes and monoterpenoids are shown in Table 1. Table 2. illustrates a variety of cyclic monoterpenes and two monoterpenoids, as characterised by their reaction products. Only reactions which produce a product ion greater than 20% of the product distribution were considered significant and are discussed. A comparison of my results with previously published data [4, 100] is also included in section 2.4.4.

2.4.1. *Monoterpene and Monoterpenoid Reactions with H_3O^+*

The most common major product ion for most of these reactions is the protonated parent compound (Table 2). This product ion is formed in excess of 60% for all monoterpenes (terpinolene, (+) limonene, (1S)-(+)-3-carene, DL-limonene) (reaction 1a) and as well as one monoterpenoid (cineole) (reaction 1b). In the case of the

monoterpenes, where the protonated parent compound is accompanied by a significant minor product ion, the minor product ion is of the formula $C_6H_9^+$ (reaction 2). The protonated parent molecule is, however, observed only as a minor product ion comprising between 30% and 36% abundance of total ion production. For example rose oxide, where two fragment ions are detected, a hydrocarbon ion is formed (reaction 3a) and hydroxide abstraction occurs (reaction 3b). In addition to protonated parent compound, several typical fragment ions are observed [88, 100].



2.4.2. Monoterpene and Monoterpenoid Reactions with NO^+

The major product ion for most of these reactions results from charge transfer, where charge transfer results for all monoterpenes (reaction 4a) and one monoterpenoid (reaction 4b). Significant minor products also accompany the charged parent compound for several standards. The minor product ion is $C_7H_9^+$ (m/z 93) for (1S)-(+)-3-carene (reaction 5) and methyl abstraction occurs for terpinolene (reaction 6) and rose oxide (reaction 7), whereas both the fragment ion and reaction process are detected for DL-limonene.

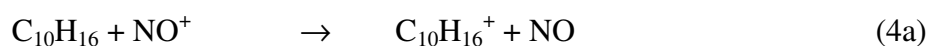


Table 1. Rate coefficients of the reactions between H_3O^+ , NO^+ and O_2^+ with a series of monoterpenes and monoterpeneoids. Estimated values and/or averages for α and μ are calculated for compounds which do not have previously recorded data and are listed in italics [53, 57, 74]. The collisional rate coefficients, k_c , in units of $10^{-9} \text{ cm}^3 \text{ s}^{-1}$, for all reactions have been calculated via the parameterized trajectory formulation by Su and Chesnavich [92] and displayed in square brackets.

| Molecule | Molecular Weight | Electric Dipole Polarizability | Dipole Moment | Rate Coefficient | | |
|--|---------------------|---|--------------------------------|---|---|--|
| | <i>m</i> (g/mol) | <i>α</i> (10^{-24} cm^3) | <i>μ</i> (D) | k_c (H_3O^+) ($10^{-9} \text{ cm}^3 \text{ s}^{-1}$) | k_c, k (NO^+) ($10^{-9} \text{ cm}^3 \text{ s}^{-1}$) | k_c, k (O_2^+) ($10^{-9} \text{ cm}^3 \text{ s}^{-1}$) |
| (+) limonene $\text{C}_{10}\text{H}_{16}$ | 136 | <i>18.65</i> | <i>1.57</i> | [3.16] | 2.70 [2.60] | 2.49 [2.53] |
| (1S)-(+)-3-carene $\text{C}_{10}\text{H}_{16}$ | 136 | <i>18.65</i> | <i>2.69</i> | [4.09] | 3.05 [3.37] | 2.92 [3.28] |
| DL-limonene $\text{C}_{10}\text{H}_{16}$ | 136 | <i>18.65</i> | <i>1.57</i> | [3.16] | 1.70 [2.60] | 1.84 [2.53] |
| terpinolene $\text{C}_{10}\text{H}_{16}$ | 136 | <i>18.65</i> | <i>1.57</i> | [3.16] | 1.94 [2.60] | 1.74 [2.53] |
| cineole $\text{C}_{10}\text{H}_{18}\text{O}$ | 154 | <i>18.63</i> | <i>2.83</i> | [4.19] | 3.87 [3.44] | 3.60 [3.35] |
| rose oxide $\text{C}_{10}\text{H}_{18}\text{O}$ | 154 | <i>18.63</i> | <i>2.95</i> | [4.31] | 2.58 [3.53] | 2.32 [3.44] |

Table 2a. Product(s) of the reactions between H_3O^+ , NO^+ and O_2^+ with a series of monoterpenes. The molecular formulae of the ion products given may not be an exact representation of their structure. The percentage of each ion product are calculated and shown in parentheses. Neutral products are listed for H_3O^+ and NO^+ and not for O_2^+ reactions because the neutral products are not easily defined.

| Molecule | H_3O^+ | NO^+ | O_2^+ |
|---|--|--|--|
| (+)-limonene $\text{C}_{10}\text{H}_{16}$ | $\text{C}_{10}\text{H}_{16}\cdot\text{H}^+$ (64) + H_2O Protonated Parent Compound | $\text{C}_{10}\text{H}_{16}^+$ (97) + NO Charge Transfer | C_7H_9^+ (27) Other (73) |
| | C_6H_9^+ (36) + $\text{C}_4\text{H}_7\cdot\text{H}$ + H_2O Hydrocarbon | Other (3) | |
| (1S)-(+)-3-carene $\text{C}_{10}\text{H}_{16}$ | $\text{C}_{10}\text{H}_{16}\cdot\text{H}^+$ (64) + H_2O Protonated Parent Compound | $\text{C}_{10}\text{H}_{16}^+$ (35) + NO Charge Transfer | C_7H_9^+ (55) Other (45) |
| | C_6H_9^+ (36) + $\text{C}_4\text{H}_7\cdot\text{H}$ + H_2O Hydrocarbon | C_7H_9^+ (35) + $\text{C}_3\text{H}_8\text{NO}$ Propyl abstraction Other (30) | |
| DL-limonene $\text{C}_{10}\text{H}_{16}$ | $\text{C}_{10}\text{H}_{16}\cdot\text{H}^+$ (70) + H_2O Protonated Parent Compound | C_7H_9^+ (50) + $\text{C}_3\text{H}_7\text{NO}$ Propyl abstraction | C_7H_9^+ (50) $\text{C}_{10}\text{H}_{16}^+$ (27) |
| | C_6H_9^+ (30) + $\text{C}_4\text{H}_7\cdot\text{H}$ + H_2O Hydrocarbon | $\text{C}_{10}\text{H}_{16}^+$ (23) + NO Charge Transfer $\text{C}_9\text{H}_{13}^+$ (21) + CH_3NO Methyl abstraction | $\text{C}_9\text{H}_{13}^+$ (23) |

Table 2a. continued.

terpinolene
C₁₀H₁₆

C₁₀H₁₆·H⁺ (100) + H₂O
Protonated Parent Compound

C₁₀H₁₆⁺ (73) + NO
Charge Transfer

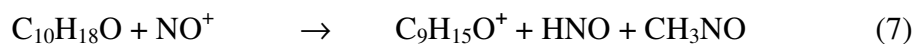
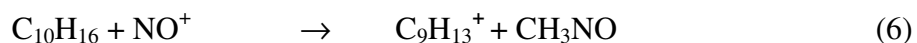
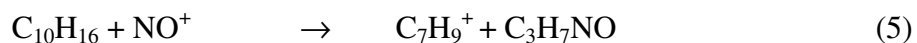
C₉H₁₃⁺ (27) + CH₃NO
Methyl abstraction

C₉H₁₃⁺ (63)

C₁₀H₁₆⁺ (37)

Table 2b. Product(s) of the reactions between H_3O^+ , NO^+ and O_2^+ with two monoterpenoids. The molecular formulae of the ion products given may not be an exact representation of their structure. The percentage of each ion product are calculated and shown in parentheses. Neutral products are listed for H_3O^+ and NO^+ and not for O_2^+ reactions because the neutral products are not easily defined.

| Molecule | H_3O^+ | NO^+ | O_2^+ |
|--|--|--|--|
| cineole $\text{C}_{10}\text{H}_{18}\text{O}$ | $\text{C}_{10}\text{H}_{18}\text{O}\cdot\text{H}^+$ (100) + H_2O Protonated Parent Compound | $\text{C}_{10}\text{H}_{18}\text{O}^+$ (52) + NO Charge Transfer Other (48) | $\text{C}_{10}\text{H}_{18}\text{O}^+$ (26) $\text{C}_9\text{H}_{15}\text{O}^+$ (20) Other (54) |
| rose oxide $\text{C}_{10}\text{H}_{18}\text{O}$ | $\text{C}_6\text{H}_{11}\text{O}^+$ (43) + $\text{C}_4\text{H}_7\cdot\text{H}$ + H_2O Carbon chain fragmentation $\text{C}_{10}\text{H}_{17}^+$ (30) + $2\text{H}_2\text{O}$ Hydroxide extraction $\text{C}_{10}\text{H}_{18}\text{O}\cdot\text{H}^+$ (27) + H_2O Protonated Parent Compound | $\text{C}_9\text{H}_{15}\text{O}^+$ (51) + CH_3NO Methyl abstraction $\text{C}_{10}\text{H}_{18}\text{O}^+$ (49) + NO Charge Transfer | $\text{C}_9\text{H}_{15}\text{O}^+$ (100) |



2.4.3. Monoterpene and Monoterpenoid Reactions with O_2^+

Many more fragment ions are detected from the reactions of O_2^+ than with H_3O^+ and NO^+ which is expected, as it has been seen in earlier work [100]. The abundance of fragment ions is attributed to the recombination energy of O_2^+ ions [52 in 100]. Several less abundant product ions (< 20% of total) of low molecular weight are detected following these reactions [100]. Similar to Wang, Španěl and Smith [100], species C_7H_9^+ (m/z 93), $\text{C}_9\text{H}_{13}^+$ (m/z 121) and $\text{C}_{10}\text{H}_{16}^+$ (m/z 136) are commonly detected in monoterpene analysis, and $\text{C}_9\text{H}_{15}\text{O}^+$ species (m/z 139) is detected in monoterpenoid analysis.

2.4.4. Comparison of Results to Previous Data

To compare rate coefficient data, previously published compounds were examined [4, 100]. Dipole moment and polarizability values are required for each specific compound to determine rate kinetics using the parameterized trajectory formula by Su and Chesnavich [92]. Rate coefficient values for the H_3O^+ precursor ion may differ due to varying sources of data used. For many of the compounds that I tested these data were not available. Thus, I developed criteria for selecting similar compounds whose data for dipole moment and polarizability were available. When similar compounds could not be found, the averaged data values for multiple ions were used. Additionally, I used the most abundant ion product from the reactions of the compound with H_3O^+ for the molecular mass value. This ion differed for cineole where my analysis

showed this ion to be the protonated parent compound (Table 2b), whereas, Amelynck *et al* reported the major reaction process as H₂O ejection after protonation resulting in C₁₀H₁₇⁺ [4].

My data generally reflects previously published works [4, 100]. Rate coefficient values were of the same magnitude overall; however, some values differed slightly. As well, I only reported ions which are in 20% abundance or greater. A more detailed comparison follows.

Overall, higher rate kinetic values were calculated and experimentally determined for (1S)-(+)-3-carene (4.09 x 10⁻⁹ cm³ s⁻¹, 3.05 x 10⁻⁹ cm³ s⁻¹ and 2.92 x 10⁻⁹ cm³ s⁻¹ with H₃O⁺, NO⁺ and O₂⁺ respectively, Table 1) when compared to 3-carene (2.6 x 10⁻⁹ cm³ s⁻¹, 2.2 x 10⁻⁹ cm³ s⁻¹ and 1.9 x 10⁻⁹ cm³ s⁻¹ with H₃O⁺, NO⁺ and O₂⁺, respectively) [100]. Two additional ions were seen on my spectra for NO⁺ analysis that were not reported by Wang, Španěl and Smith [100], C₆H₈⁺ and C₉H₁₃⁺. However, these ions represented less than 20% total ion abundance and are not reported. Also, Wang, Španěl and Smith [100], report a fragment ion at *m/z* 135. An ion peak at *m/z* 135 was seen in my spectra, however, this peak was minor and not considered for further analysis. Several unique ion peaks (C₆H₈⁺, C₇H₈⁺, C₇H₉⁺, C₉H₁₃⁺ and C₁₀H₁₆⁺), were seen using (1S)-(+)-3-carene reacted with O₂⁺ but remain unreported because these ions were below 20% abundance. Two ions, C₇H₁₀⁺ and C₈H₁₁⁺, reported by Wang, Španěl and Smith [100], were seen as minor peaks on my spectra and were not considered significant for analysis.

Similar rate kinetic data was calculated and experimentally determined for (+)-limonene and DL-limonene (Table 1) as compared to the previously published rate kinetic data for R-limonene [100]. Although, similar rate kinetic data was obtained,

differences in specific product ions were detected. The same ions result from the reactions with H_3O^+ for all three limonene isomers; however, differences can be seen for the NO^+ and O_2^+ precursor ion reactions. The (+) limonene produces a single product ion and five additional fragment ions from analysis with NO^+ and O_2^+ respectively (Table 2a). Similar to Wang, Španěl and Smith [100], NO^+ reaction produces $\text{C}_{10}\text{H}_{16}^+$ as the most abundant ion. They also report C_7H_8^+ and C_7H_9^+ as minor ions. These ions are seen in my spectra however, the peaks are too small to be included for further analysis. Ions that resulted from the O_2^+ reactions are not reported because of less than 20% abundance. DL-limonene lacks the fragment ion at C_7H_8^+ , for analysis with NO^+ and O_2^+ , but has an additional ion at $\text{C}_9\text{H}_{13}^+$ for NO^+ (Table 2a). Ion peak m/z 92 is minor when compared to other abundant ion peaks, and is not included in further analysis. Wang, Španěl and Smith also report C_7H_8^+ , in low ion abundance [100]. $\text{C}_9\text{H}_{13}^+$ is an ion fragment frequently seen in terpenes, although primarily for O_2^+ reactions. The fragment ion $\text{C}_9\text{H}_{13}^+$ appears to follow trends and be a true representation of DL-limonene in my analysis.

Terpinolene was compared to α -terpinene. These isomers differ by the positioning of one double bond. My calculations of rate kinetics for terpinolene ($3.16 \times 10^{-9} \text{cm}^3 \text{s}^{-1}$, $1.94 \times 10^{-9} \text{cm}^3 \text{s}^{-1}$ and $1.74 \times 10^{-9} \text{cm}^3 \text{s}^{-1}$ with H_3O^+ , NO^+ and O_2^+ respectively, Table 1) were similar to α -terpinene ($2.6 \times 10^{-9} \text{cm}^3 \text{s}^{-1}$, $2.0 \times 10^{-9} \text{cm}^3 \text{s}^{-1}$ and $2.0 \times 10^{-9} \text{cm}^3 \text{s}^{-1}$, with H_3O^+ , NO^+ and O_2^+ respectively) [100] and may not be useful in differentiating the two isomers. An additional ion fragment was viewed for terpinolene ($\text{C}_9\text{H}_{13}^+$, Table 2a) analysis with NO^+ . Alternatively, two additional fragment ions are reported for α -terpinene (C_7H_8^+ , C_7H_9^+) [100]. My analyses revealed a unique ion peak at m/z 121.

This fragment ion is reported in the literature for the O_2^+ precursor ion [100]. Methyl abstraction is not an uncommon reaction and the spectra resulting from Multi Ion Profile analysis shows that an ion at m/z 121 runs parallel with the ion at m/z 136, resulting from charge transfer which is a typical reaction process for terpenes with NO^+ . The ion peak at m/z 92 was not seen in my spectra and ion peak m/z 93 was considered in too low abundance to be included in further analysis. These ions are also reported in low abundance by Wang, Španěl and Smith [100], at 4% and 16% respectively.

The standard cineole provided to me by Dr. Randolph Beaudry, did not specify which isomer. This could be 1,8-, 1,4- cineole or a mixture of both. Higher rate kinetic values, by 62% for H_3O^+ and NO^+ and by 67% for O_2^+ , were calculated and experimentally determined for cineole (Table 1) when compared to 1,8-cineole [4]. Two additional fragment ions were seen for each of H_3O^+ ($C_{10}H_{17}^+$, $^*C_{10}H_{17}^+$ ($^{*13}C$ -isotope)), NO^+ ($C_{10}H_{16}^+$, $C_9H_{15}O^+$) and O_2^+ ($C_9H_{18}^+$, $C_{10}H_{16}^+$) analyses with 1,8-cineole [4]. Amelynck, *et al* [4] report fragment ions at m/z 137 and m/z 138 for 1,8-cineole analysis with H_3O^+ . Ion peaks at these m/z values were seen in my spectra as well. When analyzed using Multi Ion Profile, the spectra suggest these ions may be the formation of random adduct ions which are not true representations of the compound and are not included in my analysis. Amelynck, *et al* [4] also reported two additional ions at m/z 136 and m/z 139, produced from the reactions with NO^+ . My analysis showed minor ion peaks at these m/z values. The 136 m/z ion was in too low abundance to be included in my analysis. Amelynck, *et al* [4] also reported this ion in low abundance. Ion m/z 139 was analysed using Multi Ion Profile. Spectra from this analysis showed that the ion at m/z 139 may be the result of random adduct ion production, thus it was not included as a

relevant ion. Several minor ions reported by Amelynck, *et al* [4] are not included in my analysis due to low abundance.

As far as I am aware, rose oxide has not been previously examined using the SIFT technique, thus, data reported for this compound are original.

2.5. Concluding Remarks

As observed by Wang, Španěl and Smith [100], I have further confirmed that SIFT analyses can provide quantitation of total monoterpenes present in a sample [100]. This can be calculated by summing the major ions present that are typical of monoterpene analysis; m/z 81 and m/z 137 for H_3O^+ and m/z 93 for NO^+ [100]. I have also noted that known paired isomers, for example, (+) limonene and DL-limonene, can be differentiated by comparing the results obtained from NO^+ analysis (Table 2) [100]. When analyzing a sample using O_2^+ , several minor fragment ions are produced resulting in unsatisfactory spectra for molecule identification [100]. This is apparent for (+) limonene and (1S)-(+)-3-carene. However, typical fragment ions are detected for DL-limonene and terpinolene [100].

H_3O^+ reactions with monoterpenoids produce typical products as seen in Španěl and Smith [88]. Rose oxide produces three ionic species, which weakens the strength of a successful identification match; whereas cineole produces a single product ion for terpenoids [88]. In contrast to the general trends reported by Španěl and Smith [88], NO^+ reactions result in charge transfer and fragment ions as major products for both monoterpenoids. O_2^+ reactions produce variable results with monoterpenoids [88]. Rose oxide reaction forms a single product ion in contrast to cineole, which undergoes several processes: charge transfer, methyl abstraction and fragmentation resulting in several

minor fragment ions. Additional monoterpenoids should be analyzed to conclude that a general trend exists. This study adds supporting data on the reactions of monoterpenes and monoterpenoids to extend the library database and further enhance the information that SIFT-MS provides to analysis of volatile emissions.

2.6. Acknowledgments

I thank Dr. Randolph Beaudry from the Department of Plant and Soil Sciences, Michigan State University, for providing several of the compounds used in this study.

CHAPTER 3.0. ESTERS

3.1. Abstract

Nineteen ester compounds were examined (ethyl trans-crotonate, propyl propanoate, ethyl butanoate, methyl pentanoate, ethyl pentanoate, propyl 2-methyl propanoate, 2-methyl propyl propanoate, butyl propanoate, methyl heptanoate, 2-methyl propyl 2-methyl propanoate, 2-methyl propyl butanoate, butyl butyrate, n-butyl acetate, 2-methyl propyl acetate, 2-methyl butyl acetate, pentyl acetate, 5-hexenyl acetate, 3-hexenyl acetate and methyl salicylate) using selected ion flow tube-mass spectrometry. The H_3O^+ reactions primarily generate the protonated parent compound, $\text{R}_1\text{COOR}_2\cdot\text{H}^+$, and may also produce R_2^+ fragment ions and/or fragmentation after the alcohol, followed by hydroxide ion addition and protonation. Collisional association/adduct ions, $\text{R}_1\text{COOR}_2\cdot\text{NO}^+$, are the main products formed in the NO^+ reactions, although, the carboxyl ion fragment is also detected frequently. The identification of the parent compound may be made more easily in the H_3O^+ and NO^+ reactions. The inclusion of O_2^+ reactions in the analysis provides additional information, which may be applied when the identity of a parent compound cannot be determined solely from the H_3O^+ and NO^+ analysis. SIFT-MS provides a means of molecule detection and identification, without destroying the sample of interest. In the case of these plant-derived esters, SIFT-MS may be used to detect and identify compounds present in a plant sample of interest.

3.2. Introduction

Esters are among the most common odour and flavour chemical compounds produced by plants. They have become an important added ingredient in many food products. Commonly found in plant oils, esters emit fruity aromas and flavours which are heightened during the ripening process and are often used as criteria for food quality and ultimately, consumer preference [31, 72]. The flavour industry provides artificial aromas for flavourings to satisfy the demand of the public [97]. For example, ethyl butyrate is a popular compound which gives rise to pineapple-banana flavour [30]. This flavour is added to beverages and snacks to attract the consumer, as well as to medicines to make these appealing to young children. Strawberries are one of the most popular fruits consumed and cultivated around the world [97]. The familiar aroma of the strawberry is favoured in aroma analysis [97]. Key aroma compounds of the strawberry were quantified and defined into “aroma types” [97]. Aroma types are used to develop a criterion for quality control in strawberry breeding [97]. More than 360 volatile compounds have been identified in strawberries, including esters such as methyl butyrate, ethyl butyrate, methyl butanoate, ethyl butanoate, methyl hexanoate, ethyl hexanoate and butyl acetate [73, 97]. Esters are also important flavour compounds in Royal Gala apples. Royal Gala apples produce butyl acetate, hexyl acetate and 2-methyl butyl acetate which contribute to ripe fruit flavour [79, 106]. Volatile compounds also play an important role in proper processing techniques and food spoilage [14]. Orange juice loses desirable aroma compounds and can form “off flavours” by heating and poor storage techniques [63]. Aromatic food volatiles occur at low concentrations, but human sensory cells in the nose and throat have very low detection threshold for these compounds [31, 63]. This has

led to the common practice of using sensory panels in food quality assessment [79, 107], a practice suggested as early as Greek classical period [60]. The instrumental detection and identification of food volatiles has gained much recent interest due to the increased demand for all natural flavourings by the consumer [14, 22, 48]. The analytical devices used to carry out these analyses have been improved over the years to achieve efficient operation and to produce reproducible results [55]. With advancements made in this technology, several volatiles have been successfully and routinely identified in food products [73, 97]. On the other hand, there have been several attempts to study volatile compounds from natural products which lead to ambiguous results, either due to inadequate detection devices, or difficult compound mixtures [49, 89].

Instruments have been developed to imitate the analytical ability of the earliest detection device, the mammalian nose [60]. The most commonly used combination of techniques is gas chromatography (GC) and mass spectrometry (MS) developed in the 1950's [60]. GC encompasses all chromatographic processes in which the mobile phase is gaseous [37]. MS is used to determine the chemical arrangement of unknown substances by accurate mass determination of separated fragments [14]. The union of GC and MS permitted the identification of separated volatile compounds and has continued to be used as a traditional mode of food flavour analysis [60, 95]. Although, GC-MS remains a useful analytical instrument, there are problems associated with this technique for odour analysis. The sample must be extracted in liquid form prior to volatilization and subsequent analysis. For example, in liquid-liquid extractions, lipids and carotenoids are extracted together with the desired volatile compounds [63]. These non-volatile compounds can break down in the GC injector and produce artefacts compromising the

GC column [63]. Generally, sample mixtures analyzed using GC-MS tend to be very complex. Ideal separation is often not achieved because of the complexity of the samples and/or because increased speed of the chromatographic runs is favoured [5]. Also, compounds with similar mass spectra may be co-eluted preventing the identification of the desired compound [29]. Databases provided by instrument manufacturers are often inadequate at providing valid compound identification [5]. Lastly, compounds occurring at low concentrations may remain undetected.

Consumer demand for natural flavouring substances, rather than synthetic flavour compounds, has flooded the flavour market [22]. As a result of technological advancements, extensive lists of volatiles in foods have been reported [73, 99]. Of the hundreds of volatile compounds present in a food item, only few supply odour and aroma [33, 99]. The ability to differentiate between odour active compounds from a range of volatiles in a food product is critical in flavour analysis [99]. Past efforts to develop instrumental olfactory systems have been inadequate. Quantitative analyses required specific sensors for individual odour compounds, resulting in difficult and expensive analyses [95]. In 1964, Fuller, Steltenkamp and Tisserand [27] introduced gas chromatography-olfactometry (GC-O) for the study of aromatic volatile compounds. This combines the instrumental separation method (GC) with the sensitive olfactory detection of the human nose. GC-O has been used as an effective means for complex volatile mixture analysis [27, 99]. Although GC-O has potential to be a successful diagnostic tool, it is not without problems. Single compounds were examined, reproducibility was a major issue due to the physically difficult analyses of the hot dry effluent by the assessor and adequate data can not be attained from a single run [71, 99].

Modifications have been made to early devices with the development of new technology [95].

Further attempts to develop purely instrumental analysis of aroma compounds continue. Headspace analysis (replacing solvent extraction) gained in popularity because only volatiles are collected, reducing column damage and artifacts [63]. A new commonly used gas phase detector is atmospheric pressure ionization-mass spectrometer (API-MS) [22, 89]. In API-MS, a liquid sample is vaporized then subsequent ionization occurs at atmospheric pressure via ion molecule reactions followed by detection via a quadrupole mass analyzer [40]. However, API-MS lacks separation ability for several compounds, interpretation of mass spectra is complicated and quantification of individual volatiles in a mixture is difficult [89, 94].

The selected ion flow tube (SIFT) analytical method allows real-time analysis for the monitoring of complex mixtures. This method does not require the isolation or purification of volatile compounds and rapidly analyzes *in vivo* spectral compounds simultaneously [80]. The SIFT technique was developed in the 1970s by D. Smith and N.G. Adams to study ion molecule reactions in the gas phase at thermal energies and is now a standardized method for trace gas analysis [3]. This technique is well suited for the rapid detection and quantification of volatile organic compounds (VOCs) [50, 100]. Selected ion flow tube-mass spectrometry (SIFT-MS) is a chemical ionization separation technique coupled to a mass spectrometer dependent on kinetic constants and ionization rates of specific VOCs [78]. H_3O^+ , NO^+ and O_2^+ , were experimentally found to be the only useable reactive precursor ions [81, 82]. These ions may be introduced simultaneously or individually to react with unknown volatile compounds to produce

secondary ions identifiable by mass analysis and quantified using the determination of the rate of the reaction [76].

SIFT-MS will be utilized to develop a data library of real time analysis of mass spectra of individual compounds. In this report I focus on esters. These mass spectra will ultimately be correlated with real time spectra of actual plant material. The current study focuses on the results of the reactions between H_3O^+ , NO^+ and O_2^+ with a series of esters.

3.3. Experimental Section

I adopted SIFT-MS methodology developed by Adams and Smith [3] as described in chapter 2 section 2.3. A detailed summary of SIFT-MS has previously been reported [75, 78, 83, 84, 86].

3.3.1. Data Acquisition

Data acquisition was performed as described in chapter 2 section 2.3.1.

3.3.2. Data Handling and Display

Data handling and display was performed as described in chapter 2 section 2.3.2.

3.4. Results and Discussion

Calculated k_c for the H_3O^+ proton transfer reactions and the experimentally determined k with k_c for the NO^+ and O_2^+ reactions with 18 esters and methyl salicylate are shown (Table 3), as well as likely products of ionic reaction which produce a product ion with > 20 % abundance are shown (Table 4). In the event where a product ion could potentially contain an oxygen atom (carboxyl ion) or not (hydrocarbon ion), the presence

Table 3. Rate coefficients of the reactions between H_3O^+ , NO^+ and O_2^+ with a series of esters. Estimated values and/or averages for α and μ are calculated for compounds which do not have previously recorded data and are listed in italics [53, 57, 74]. The collisional rate coefficients, k_c , in units of $10^{-9} \text{ cm}^3 \text{ s}^{-1}$, for all reactions have been calculated via the parameterized trajectory formulation by Su and Chesnavich [92] and displayed in square brackets.

| Molecule | Molecular Weight | Electric Dipole Polarizability | Dipole Moment | Rate Coefficient | | |
|--|---------------------|---|--------------------------------|---|---|--|
| | <i>m</i> (g/mol) | <i>α</i> (10^{-24} cm^3) | <i>μ</i> (D) | k_c (H_3O^+) ($10^{-9} \text{ cm}^3 \text{ s}^{-1}$) | k_c, k (NO^+) ($10^{-9} \text{ cm}^3 \text{ s}^{-1}$) | k_c, k (O_2^+) ($10^{-9} \text{ cm}^3 \text{ s}^{-1}$) |
| ethyl trans-crotonate $\text{CH}_3\text{CH}=\text{CHCOOC}_2\text{H}_5$ | 114 | <i>14.2</i> | <i>(1.74)</i> | [3.06] | 1.88 [2.53] | 2.31 [2.47] |
| propyl propanoate $\text{C}_2\text{H}_5\text{COOC}_3\text{H}_7$ | 116 | <i>14.2</i> | 1.79 ± 0.03 | [3.10] | 1.66 [2.56] | 1.75 [2.50] |
| ethyl butanoate $\text{C}_3\text{H}_7\text{COOC}_2\text{H}_5$ | 116 | <i>14.2</i> | <i>(1.74)</i> | [3.07] | 2.89 [2.54] | 3.05 [2.47] |
| methyl pentanoate $\text{C}_4\text{H}_9\text{COOCH}_3$ | 116 | <i>14.2</i> | 1.61 ± 0.03 | [2.96] | 0.35 [2.45] | 0.58 [2.38] |
| ethyl pentanoate $\text{C}_4\text{H}_9\text{COOC}_2\text{H}_5$ | 130 | <i>14.9</i> | 1.76 | [3.09] | 1.64 [2.55] | 1.87 [2.48] |
| propyl 2-methyl propanoate $\text{CH}_3\text{CH}(\text{CH}_3)\text{COOC}_3\text{H}_7$ | 130 | <i>14.9</i> | <i>(1.86)</i> | [3.17] | 2.64 [2.62] | 2.67 [2.55] |

Table 3. continued.

| | | | | | | |
|--|-----|------|--------|--------|-------------|-------------|
| 2-methyl propyl propanoate $C_2H_5COOCH_2CH(CH_3)CH_3$ | 130 | 14.9 | (1.86) | [3.17] | 1.15 [2.62] | 1.01 [2.55] |
| butyl propanoate $C_2H_5COOC_4H_9$ | 130 | 14.9 | 1.82 | [3.14] | 1.67 [2.59] | 1.47 [2.52] |
| methyl heptanoate $C_6H_{13}COOCH_3$ | 144 | 17.2 | 1.80 | [3.23] | 2.36 [2.65] | 1.97 [2.59] |
| 2-methyl propyl 2-methyl propanoate $CH_3CH(CH_3)COOCH_2CH(CH_3)CH_3$ | 144 | 17.2 | (1.9) | [3.31] | 2.28 [2.72] | 1.81 [2.65] |
| 2-methyl propyl butanoate $C_3H_7COOCH_2CH(CH_3)CH_3$ | 144 | 17.2 | (1.9) | [3.31] | 0.13 [2.72] | 0.73 [2.65] |
| butyl butyrate $C_3H_7COOC_4H_9$ | 144 | 17.2 | 2.12 | [3.49] | 3.42 [2.87] | 2.90 [2.79] |
| n-butyl acetate $CH_3COOC_4H_9$ | 116 | 14.2 | (1.87) | [3.17] | 2.10 [2.62] | 2.20 [2.55] |
| 2-methyl propyl acetate $CH_3COOCH_2CH(CH_3)CH_3$ | 116 | 14.2 | (1.87) | [3.17] | 2.72 [2.62] | 2.67 [2.55] |

Table 3. continued.

| | | | | | | |
|---|-----|------|-----------------|--------|-------------|-------------|
| 2-methyl butyl acetate $\text{CH}_3\text{COOCH}_2\text{CH}(\text{CH}_3)\text{C}_2\text{H}_5$ | 130 | 14.2 | (1.86) | [3.13] | 2.63 [2.58] | 2.55 [2.52] |
| pentyl acetate $\text{CH}_3\text{COOC}_5\text{C}_{11}$ | 130 | 14.9 | 1.75 ± 0.01 | [3.08] | 1.45 [2.54] | 1.21 [2.48] |
| 5-hexenyl acetate $\text{CH}_3\text{COOC}_4\text{H}_2\text{CH}=\text{CH}_2$ | 142 | 17.2 | 1.80 | [3.23] | 2.80 [2.66] | 2.74 [2.59] |
| 3-hexenyl acetate $\text{CH}_3\text{COOC}_2\text{H}_4\text{CH}=\text{CHC}_2\text{H}_5$ | 142 | 17.2 | 1.80 | [3.23] | 3.12 [2.66] | 2.62 [2.59] |
| methyl salicylate $\text{C}_6\text{H}_4(\text{HO})\text{COOCH}_3$ | 152 | 16.9 | 2.47 | [3.78] | 2.72 [3.11] | 3.05 [3.02] |

Table 4. Product(s) of the reactions between H_3O^+ , NO^+ and O_2^+ with a series of esters. The molecular formulae of the ion products given may not be an exact representation of their structure. The percentage of each ion product are calculated and shown in parentheses. Neutral products are listed for H_3O^+ and NO^+ and not for O_2^+ reactions because the neutral products are not easily defined.

| Molecule | H_3O^+ | NO^+ | O_2^+ |
|---|--|---|--|
| ethyl <i>trans</i> -crotonate $\text{CH}_3\text{CH}=\text{CHCOOC}_2\text{H}_5$ | $\text{CH}_3\text{CH}=\text{CHCOOC}_2\text{H}_5 \cdot \text{H}^+$ (100) + H_2O Protonated parent compound | $\text{CH}_3\text{CH}=\text{CHCO}^+$ (75) + $\text{C}_2\text{H}_5\text{NO}_2$ Carboxyl ion Other (25) | $\text{CH}_3\text{CH}=\text{CHCOOCH}_2^+$ (49) Methyl abstraction $\text{CH}_3\text{CH}=\text{CHCO}^+$ (33) Carboxyl ion Other (18) |
| propyl propanoate $\text{C}_2\text{H}_5\text{COOC}_3\text{H}_7$ | $\text{C}_2\text{H}_5\text{COOC}_3\text{H}_7 \cdot \text{H}^+$ (81) + H_2O Protonated parent compound Other (19) | $\text{NO}^+ \cdot \text{C}_2\text{H}_5\text{COOC}_3\text{H}_7$ (70) Collissional (three body) association $\text{C}_2\text{H}_5\text{CO}^+$ (30) + $\text{C}_3\text{H}_7\text{NO}_2$ Carboxyl ion | $\text{C}_2\text{H}_5\text{CO}^+$ (100) Carboxyl ion |
| ethyl butanoate $\text{C}_3\text{H}_7\text{COOC}_2\text{H}_5$ | $\text{C}_3\text{H}_7\text{COOC}_2\text{H}_5 \cdot \text{H}^+$ (100) + H_2O Protonated parent compound | $\text{C}_3\text{H}_7\text{CO}^+$ (54) + $\text{C}_2\text{H}_5\text{NO}_2$ Carboxyl ion $\text{NO}^+ \cdot \text{C}_3\text{H}_7\text{COOC}_2\text{H}_5$ (46) Collissional (three body) association | $\text{C}_3\text{H}_7\text{CO}^+$ (73) Carboxyl ion $\text{C}_3\text{H}_7\text{COOC}_2\text{H}_5^+$ (27) Charge transfer |

Table 4. continued.

| | | | |
|---|--|---|---|
| methyl pentanoate $C_4H_9COOCH_3$ | $C_4H_9COOCH_3 \cdot H^+$ (100) + H_2O Protonated parent compound | $C_4H_9CO^+$ (57) + CH_3NO_2 Carboxyl ion | $C_4H_9CO^+$ (70) Carboxyl ion |
| | | $NO^+ \cdot C_4H_9COOCH_3$ (43) Collissional (three body) association | $CH_3OCC_2H_4^+$ (30) Carbon chain fragment |
| ethyl pentanoate $C_4H_9COOC_2H_5$ | $C_4H_9COOC_2H_5 \cdot H^+$ (98) + H_2O Protonated parent compound | $C_4H_9CO^+$ (97) + $C_2H_5NO_2$ Carboxyl ion | $C_4H_9CO^+$ (51) Carboxyl ion |
| | Other (2) | Other (3) | $C_4H_9COO^+$ (30) Other (18) |
| propyl 2-methyl propanoate $CH_3CH(CH_3)COOC_3H_7$ | $CH_3CH(CH_3)COOC_3H_7 \cdot H^+$ (78) + H_2O Protonated parent compound | $CH_3CH(CH_3)CO^+$ (47) + $CH_3CH_7NO_2$ Carboxyl ion | $CH_3CH(CH_3)CO^+$ (100) Carboxyl ion |
| | $CH_3CH(CH_3)^+$ (22) + H_2O + C_3H_7OOCH Hydrocarbon | $NO^+ \cdot C_3H_7COOC_3H_7$ (42) Collissional (three body) association | |
| 2-methyl propyl propanoate $C_2H_5COOCH_2CH(CH_3)CH_3$ | $CH_3CH(CH_3)CH_2^+$ (47) + H_2O + C_2H_5COOH Hydrocarbon | $NO^+ \cdot C_2H_5COOCH_2CH(CH_3)CH_3$ (66) Collissional (three body) association | $CH_3CH(CH_3)CH^+$ (62) Hydrocarbon |
| | $C_2H_5COOCH_2CH(CH_3)CH_3 \cdot H^+$ (31) + H_2O Protonated Parent Compound | $CH_3CH(CH_3)CH_2^+$ (34) + C_2H_5COONO Hydrocarbon | $CH_3CH(CH_3)CH_2^+$ (36) Hydrocarbon |
| | $C_2H_5COOH \cdot H^+$ (21) + H_2O + $CH_3CH(CH_3)CH_2^+$ Fragment after the alcohol, OH formed, then protonated | | |

Table 4. continued.

| | | | |
|--|--|--|--|
| butyl propanoate $C_2H_5COOC_4H_9$ | $C_2H_5COOC_4H_9 \cdot H^+$ (74) + H_2O Protonated Parent Compound | $C_4H_8^+$ (40) + HNO + C_2H_5COONO Hydrocarbon | $C_4H_8^+$ (72) Hydrocarbon |
| | $C_2H_5COOH \cdot H^+$ (26) + H_2O + $C_4H_9^+$ Fragment after the alcohol, OH formed, then protonated | $NO^+ \cdot C_2H_5COOC_4H_9$ (39) Collissional (three body) association | $C_4H_9^+$ (28) Hydrocarbon |
| | | $C_4H_9^+$ (21) + C_2H_5COONO Hydrocarbon | |
| methyl heptanoate $C_6H_{13}COOCH_3$ | $C_6H_{13}COOCH_3 \cdot H^+$ (69) + H_2O Protonated Parent Compound | $C_6H_{13}CO^+$ (96) + CH_3NO_2 Carboxyl ion | $CH_3OCC_2H_4^+$ (71) Fragment |
| | $C_6H_{13}COOCH_3 \cdot H_3O^+$ (31) Collissional (three body) association | Other (4) | $C_6H_{13}CO^+$ (48) Carboxyl ion |
| | | | Other (11) |
| 2-methyl propyl 2-methyl propanoate $CH_3CH(CH_3)COOCH_2CH(CH_3)CH_3$ | $CH_3CH(CH_3)COOCH_2CH(CH_3)CH_3 \cdot H^+$ (50) + H_2O Protonated Parent Compound | $NO^+ \cdot CH_3CH(CH_3)COOCH_2CH(CH_3)CH_3$ (100) Collissional (three body) association | $CH_3CH(CH_3)CH^+$ (58) Hydrocarbon |
| | $CH_3CH(CH_3)CH_2^+$ (28) + $CH_3CH(CH_3)COO \cdot H$ + H_2O Hydrocarbon | | $CH_3CH(CH_3)CO^+$ (41) Carboxyl ion |
| | $CH_3CH(CH_3)COO \cdot 2H^+$ (22) + H_2O + $CH_3CH(CH_3)CH_2^+$ Fragment after the alcohol, OH formed, then protonated | | |

Table 4. continued.

| | | | |
|--|--|--|---|
| 2-methyl propyl butanoate $C_3H_7COOCH_2CH(CH_3)CH_3$ | $C_3H_7COOCH_2CH(CH_3)CH_3 \cdot H^+$ (96) + H_2O Protonated Parent Compound Other (4) | $NO^+ \cdot C_3H_7COOCH_2CH(CH_3)CH_3$ (68) Collissional (three body) association $C_3H_7CO^+$ (32) + $CH_3CH(CH_3)CH_2NO_2$ Carboxyl ion | $CH_3CH(CH_3)CH^+$ (58) Hydrocarbon $C_3H_7CO^+$ (40) Carboxyl ion Other (2) |
| butyl butyrate $CH_3(CH_2)_2COOC_4H_9$ | $CH_3(CH_2)_2COOC_4H_9 \cdot H^+$ (100) + H_2O Protonated Parent Compound | $C_4H_8^+$ (62) + HNO + $C_4H_9NO_2$ Hydrocarbon $CH_3(CH_2)_2CO^+$ (38) + $C_4H_9NO_2$ Carboxyl ion | $C_4H_8^+$ (72) Hydrocarbon $CH_3(CH_2)_2CO^+$ (28) Carboxyl ion |
| n-butyl acetate $CH_3COOC_4H_9$ | $CH_3COOC_4H_9 \cdot H^+$ (44) + H_2O Protonated Parent Compound $CH_3COOH \cdot H^+$ (41) + $2H_2O$ + $C_4H_9^+$ Fragment after the alcohol, OH formed, then protonated Other (15) | $NO^+ \cdot CH_3COOC_4H_9$ (100) Collissional (three body) association | $C_4H_8^+$ (82) Hydrocarbon Other (19) |
| 2-methyl propyl acetate $CH_3COOCH_2CH(CH_3)_2$ | $CH_3COOCH_2CH(CH_3)_2 \cdot H^+$ (100) + H_2O Protonated Parent Compound | $NO^+ \cdot CH_3COOCH_2CH(CH_3)_2$ (89) Collissional (three body) association Other (11) | $C_4H_8^+$ (81) Hydrocarbon Other (19) |

Table 4. continued.

| | | | |
|---|--|---|--|
| 2-methyl butyl acetate $\text{CH}_3\text{COOCH}_2\text{CH}(\text{CH}_3)\text{C}_2\text{H}_5$ | $\text{C}_2\text{H}_5\text{CH}(\text{CH}_3)\text{CH}_2^+$ (46) + H_2O + $\text{CH}_3\text{COO}\cdot\text{H}$ Hydrocarbon $\text{CH}_3\text{COOH}\cdot\text{H}^+$ (33) + $2\text{H}_2\text{O}$ + $\text{C}_2\text{H}_5\text{CH}(\text{CH}_3)\text{CH}_2^+$ Fragment after the alcohol, OH formed, then protonated | $\text{NO}^+\cdot\text{CH}_3\text{COOCH}_2\text{CH}(\text{CH}_3)\text{C}_2\text{H}_5$ (100) Collissional (three body) association | $\text{C}_5\text{H}_{10}^+$ (98) Hydrocarbon Other (2) |
| pentyl acetate $\text{CH}_3\text{COOC}_5\text{H}_{11}$ | $\text{CH}_3\text{COOC}_5\text{H}_{11}\cdot\text{H}^+$ (61) + H_2O Protonated Parent Compound $\text{CH}_3\text{COOC}_5\text{H}_{11}\cdot\text{H}_3\text{O}^+$ (27) Collissional (three body) association and deprotonated Other (13) | $\text{NO}^+\cdot\text{CH}_3\text{COOC}_5\text{C}_{11}$ (100) Collissional (three body) association | $\text{C}_5\text{H}_{10}^+$ (99) Hydrocarbon Other (1) |
| 5-hexenyl acetate $\text{CH}_3\text{COO}(\text{CH}_2)_4\text{CH}=\text{CH}_2$ | $\text{CH}_2=\text{CH}(\text{CH}_2)_4$ (67) + H_2O + $\text{CH}_3\text{COO}\cdot\text{H}$ Hydrocarbon $\text{CH}_3\text{COOC}_4\text{H}_2\text{CH}=\text{CH}_2\cdot\text{H}^+$ (33) + H_2O Protonated Parent Compound | $\text{CH}_2=\text{CHC}_3\text{H}_6\text{CH}^+$ (100)+ HNO + CH_3COONO Hydrocarbon | $\text{CH}_2=\text{CHC}_3\text{H}_6\text{CH}^+$ (47) Hydrocarbon $\text{CH}_2=\text{CHC}_2\text{H}_3^+$ (36) Hydrocarbon Other (16) |

Table 4. continued.

| | | | |
|---|--|---|--|
| 3-hexenyl acetate $\text{CH}_3\text{COO}(\text{CH}_2)_2\text{CH}=\text{CHC}_2\text{H}_5$ | $\text{C}_2\text{H}_5\text{CH}=\text{CHC}_2\text{H}_4^+$ (83) + H_2O + $\text{CH}_3\text{COO}\cdot\text{H}$ Hydrocarbon Other (17) | $\text{C}_2\text{H}_5\text{CH}=\text{CHC}_2\text{H}_3^+$ (92) + HNO + CH_3COONO Hydrocarbon deprotonated | $\text{C}_6\text{H}_{10}^+$ (83) Hydrocarbon Other (17) |
| methyl salicylate $\text{C}_6\text{H}_4(\text{HO})\text{COOCH}_3$ | $\text{C}_6\text{H}_4(\text{HO})\text{COOCH}_3\cdot\text{H}^+$ (100) + H_2O Protonated Parent Compound | $\text{C}_6\text{H}_4(\text{HO})\text{COOCH}_3^+$ (100) + NO Charge transfer | $\text{C}_6\text{H}_4(\text{HO})\text{COOCH}_3^+$ (93) Charge transfer Other (7) |

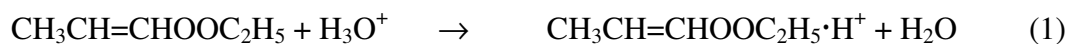
(or absence) of the oxygen atom was determined by isotope analysis.

As far as I am aware, there is no information on possible stereoisomers in the published report on esters, thus, I assume most of my information is novel. Španěl and Smith have previously reported data on several esters including, methyl formate, ethyl formate, methyl acetate, ethyl acetate, methyl propionate, ethyl propionate, methyl butyrate and methyl benzoate [87]. The following is a discussion of the H_3O^+ , NO^+ and O_2^+ reactions with additional esters.

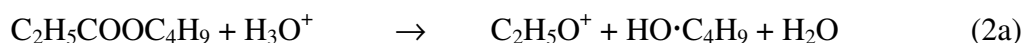
3.4.1. Ester Reactions with H_3O^+

The protonated parent molecule is produced for all reactions, with the exception of 3-hexenyl acetate (Table 4). It is the sole ion formed or the only significant ion detected in excess of 80% for fifteen esters (ethyl *trans*-crotonate, ethyl butanoate, methyl pentanoate, butyl butyrate, 2-methyl propyl acetate, methyl salicylate, propyl propanoate, ethyl pentanoate and 2-methyl propyl butanoate) (reaction 1). The protonated parent compound may be accompanied by significant minor product ions. For example, fragmentation may occur after the alkoxy oxygen (reaction 2a) and undergo hydroxide ion addition and protonation (butyl propanoate, n-butyl acetate and propyl acetate) (reaction 2b). For three branched esters, the above mentioned product ion and a hydrocarbon are produced (2-methyl propyl propanoate, 2-methyl propyl 2-methyl propanoate and 2-methyl butyl acetate) (reaction 3), while three esters, two with a double bond (5-hexenyl acetate and 3-hexenyl acetate) and one branched ester (propyl 2-methyl propanoate), produce a hydrocarbon in addition to the protonated parent compound. In two unique cases, collisional association is seen as a significant product ion (pentyl acetate and methyl heptanoate) (reaction 4).

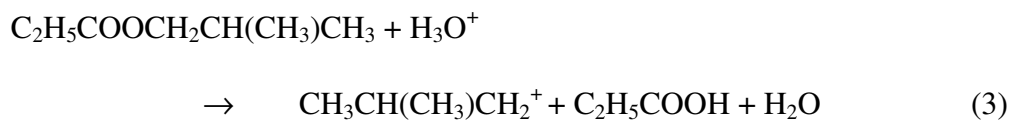
The following example of the protonated parent compound is shown using ethyl *trans*-crotonate (reaction 1).



The following example of fragmentation after the alcohol is formed (reaction 2a) followed by hydroxide addition and protonation (reaction 2b) is shown using butyl propanoate.



The following example of a hydrocarbon product is shown using 2-methyl propyl propanoate (reaction 3).



The following example of collisional association is shown using methyl heptanoate (reaction 4).

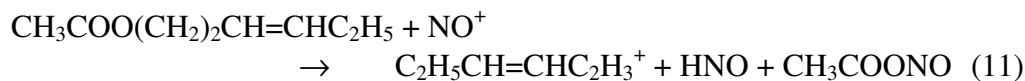
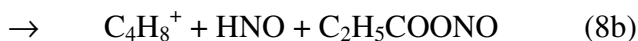
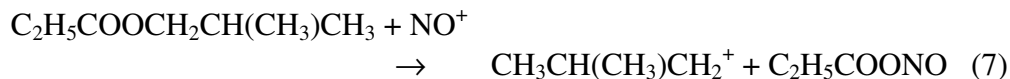


3.4.2. Ester Reactions with NO^+

The NO^+ reactions result in product ions which resemble those obtained by Španěl and Smith [87]. Collisional association (reaction 5) and R_1CO^+ carboxyl ion fragmentation (reaction 6) are observed in most ester- NO^+ reactions. However, the reactions for five esters (2-methyl propyl propanoate, butyl propanoate, butyl butyrate, 5-hexenyl acetate and 3-hexenyl acetate) result in the production of various hydrocarbons (reactions 7 to 11). The above mentioned product ions are the only significant resulting ions for the linear esters. An exception is observed for the cyclical ester (methyl

salicylate), where charge transfer is the only significant reaction observed (reaction 12).

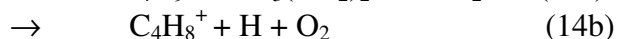
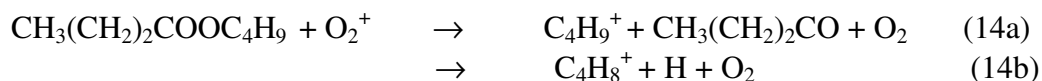
The following example of collisional association and carboxyl ion fragmentation are shown using propyl propanoate (reactions 5 to 6).



3.4.3. Ester Reactions with O_2^+

Many of the O_2^+ reaction results are similar to those observed by Španěl and Smith [87]. The parent compound is observed as a minority product, often less than 20% of the total ion content. Multiple fragmentation ions are also produced. Common fragments are R_1CO^+ , carbonyl ion (reaction 13) and various hydrocarbons, for example the deprotonated carbon chain after the fragmentation, (reactions 14a to 14b), as seen for butyl butyrate.





3.5. Concluding Remarks

This study continues to add supporting data on the reactions of esters to expand the library database and broaden the experimental evidence that SIFT-MS is a technique to study volatile compounds emitted from biological sources. The database of standard SIFT-MS spectra has been expanded with 19 new esters not previously reported. The protonated parent compound is a major product ion viewed for most ester- H_3O^+ reactions, while the R_2^+ fragment ion is often observed as a minor (or at times major) product ion resulting from these reactions as well [87]. As previously demonstrated, NO^+ reactions produce adduct ions $\text{NO}^+\cdot\text{M}$ [87], with carboxyl ion fragments also in abundance and occasionally a hydrocarbon/ R_2 fragment. O_2^+ reactions result in various fragmentation of the parent compound [87], thus, it is difficult to conclude the identity of a compound using O_2^+ as the sole means of analysis. However, O_2^+ is useful as a method to cross reference results that may be uncertain using H_3O^+ and NO^+ precursor ions alone [42].

3.6. Acknowledgments

I thank Dr. Randolph Beaudry from the Department of Plant and Soil Sciences, Michigan State University, for providing several of the compounds used in this study.

**PART II. SIFT-MS IDENTIFICATION OF SELECTED VOLATILE ORGANIC
COMPOUNDS EMITTED FROM *POLYGALA SENEGA*, *VALERIANA
OFFICINALIS* AND *CANNABIS SATIVA***

CHAPTER 4.0. APPLICATION OF SIFT-MS TECHNOLOGY

4.1. Abstract

The utility of selected ion flow tube-mass spectrometry in plant biology was studied by examining *Polygala senega*, *Valeriana officinalis* and *Cannabis sativa* volatile emissions. Few known compounds from these plant samples are detected by SIFT-MS: hexanoic acid and methyl salicylate from *Polygala senega*, ocimene from *Cannabis sativa* leaves and β -pinene and myrcene from *Cannabis sativa* seeds. Compounds unique to *Valeriana officinalis* could not be detected due to their high molecular weight, which limits volatility. The detection of several compounds cannot be confirmed due to uncertainties in the data. The SIFT-MS approach to plant volatile emissions shows some promise, however, further corroboration with GC-MS is required to compliment initial plant VOC studies.

4.2. Introduction

The search for new biologically active compounds as potential drugs is a difficult task, which requires the contribution of many scientific fields: chemistry, pharmacology and clinical sciences [13, 23]. Natural products, in particular those from known medicinal plants, are an important potential source of new drugs and new chemical entities (NCEs) [7, 13, 59]. By examining plants traditionally used as medicines, compounds which show biological activity are often isolated [13, 106]. These studies have uncovered many compounds which are commonly used as drugs today. The classical examples include the commonly used aspirin (acetylsalicylic acid) which was derived from chemical compounds isolated from *Salix sp.* [56], morphine developed from opium extracted from *Papaver somniferum* [13, 21] and anti-cancer drug paclitaxel from *Taxus brevifolia* [65, 106].

Natural products are often used as the foundation for new synthetic compounds; however, the diverse structure of natural compounds makes selection of likely candidate structures a difficult task [7, 20, 64]. Between 1981 and 2002, an estimated 28% of new NCEs were natural products or natural product-derived [7, 59]. One quarter of the world's best-selling drugs in use between 2001 and 2002 [7, 13] and 50% of new antibiotics approved by the Food and Drug Administration (FDA), were extracted from natural sources or synthesized from a known natural product [59, 106]. Historically, natural compounds and synthetic compounds occupied two different categories of chemistry [13]. This difference in approach is currently breaking down, by screening of compound libraries based on chemically modified natural product extracts [13].

I have selected for my study three plants locally available for testing, which show

potential for commercial development. These plants, *Polygala senega*, *Valeriana officinalis* and *Cannabis sativa*, are of interest because of their past medicinal use and production of volatile aromatic compounds, which are amenable for analysis by SIFT-MS (discussed below). A brief introduction to each selected plant species follows the introduction to SIFT-MS.

4.2.1. Selected ion flow tube-mass spectrometry

Selected ion flow tube-mass spectrometry (SIFT-MS) was introduced in section 2.3. To recapitulate briefly, the technique was developed in the 1970s by D. Smith and N.G. Adams and is now standardized method for trace gas analysis [3, 49, 100]. SIFT-MS is one of the most reliable techniques available for the study of kinetics and ionic reactions and ideally suited for the rapid detection and quantification of volatile organic compounds [3, 49, 100]. H_3O^+ , NO^+ and O_2^+ , are the only useable reactive precursor ions used in analyses to produce identifiable secondary ions [76, 81, 82]. The potential contribution of SIFT-MS to natural product research correlating data library product ions with real time spectra of actual plant material will be further tested in this work using the gaseous headspace above model plants, *Polygala senega*, *Valeriana officinalis* and *Cannabis sativa*. Further refinement and computer aided identification of SIFT-MS signals may lead to the identification and rapid analysis of potentially useful plant products.

4.2.2. *Polygala senega*

Polygala senega is a perennial herb, indigenous to North America, the Canadian prairies in particular [46, 96]. The visible portion of the herb consists of green to purplish

lance-shaped leaves ending in an elongated spike of green-white or pink-white flowers. Its underground parts consist of several vertically oriented shoots, branched off from a single dominant crown root [96]. Due to the similarity in appearance of the root to that of a snake, native peoples initially administered *Polygala senega* as a snake bite remedy by applying a macerate of the roots to the affected area [46]. This plant was later used as a general remedy by several native tribes for a multitude of ailments such as congestion, coughs, sore throats, earaches and skin lesions [91, 96]. *Polygala senega* enhances immune response to proteins and viral agents, which may attribute to the success of the plant as a general therapeutic [25]. During the 1730s, John Tennent, a Scottish physician practicing in New England, observed that the symptoms experienced by patients in the later stages of pneumonia and pleurisy were similar to the symptoms experienced by persons suffering from snake bites [96]. He later came to the realization that *Polygala senega* could also be useful to those suffering from the aforementioned disorders. In the 1800's, *Polygala senega* gained the interest of the European medical profession as potential treatments for pleurisy and pneumonia [10, 46, 96]. This plant continues to be a traditional herb of great interest [96]. In order to ensure the wild population is not depleted, the herb is ethically harvested in Manitoba and Saskatchewan and attempts at cultivation are being made [25].

4.2.3. *Valeriana officinalis*

Valeriana officinalis is a herbaceous, perennial herb native to North America, Asia and Europe [32, 35]. Beginning as a short rhizome, *Valeriana* can reach heights of up to two meters [69]. The herb flowers, producing a cluster of white or pink petals with lance shaped leaves [69]. The roots and rhizomes of *Valeriana officinalis* L. contain the

drug valerian which has a long history of use in traditional medicine since it was described by the ancient Greeks and Romans as a sedative [19, 28]. Although, *Valeriana* was and currently is primarily used as a sedative to treat insomnia, it has been also been prepared for oral administration to treat disorders such as hypertension, angina, palpitation, anxiety, gastro-intestinal spasm, among other ailments [39, 41, 47 and 61 in 19, 24, 35]. *Valeriana officinalis* L. continues to be cultivated on a commercial scale and remains published in several pharmacopeias [32]. In addition to its traditional medicinal value, *Valeriana* is also used in combination with other herbs as natural insect and pest repellent [40]. The popularity of this species continues to grow with the use of essential oil extracts in modern consumer products such as cosmetics and aromatherapy products [50].

4.2.4. *Cannabis sativa*

Cannabis sativa is well known as marijuana or industrial hemp. It has been cultivated for more than 5000 years all over the world and its resin has been used for its euphoric effect since ancient times [58, 68]. Recordings of *Cannabis* use dates back to Avesta, the sacred book of knowledge of the Zoroastrian faith, 1000-600 B. C. [58]. Although popularized as a recreational drug, *Cannabis* possesses beneficial medicinal qualities largely due to psychoactive, analgesic and sedative properties of THC (tetrahydrocannabinol) [45, 58, 102]. The use of *Cannabis* as a medication remains popular in India and it has become recognized and prescribed as an effective therapeutic treatment in Western medicine for illnesses which cause severe pain or discomfort such as rheumatoid arthritis, multiple sclerosis and acquired immune deficiency syndrome (AIDS) [18, 58, 68, 104, 105]. Extracts from the plant have also

been found to possess antibacterial properties against gram-positive bacteria, as well as insecticidal properties [26, 44, 98].

The use of *Cannabis* extends beyond medicinal applications. Typically, *Cannabis* varieties lacking THC (referred to as industrial hemp) have a more robust stalk and are used as a fiber source. Historically, *Cannabis* fibers have been used in a number of items such as nets, rope, textiles, paper and fuel and are currently becoming regular ingredients in common household items such as insulation and cosmetic products [66, 68, 104]. *Cannabis* seeds also provide an excellent source of edible oil, fiber and protein [15].

The top portion of a female plant is covered with glandular hairs that secrete resin which functions as a protective barrier over seeds during ripening [58]. During resin gland development, cannabinoids and associated terpenes are synthesized [93]. The resin is mainly composed of cannabinoids which are of medicinal value [93]. *Cannabinoids* are not aromatic, thus associated terpenes provide the fragrant odours which are characteristic of *Cannabis* essential oils [67]. Low THC, or industrial hemp was used in my experiments. Identified by GC methods, Rothschild, Bergstrom and Wangberg [68] and Ross and ElSohy [67], found that volatile emissions of *Cannabis* consist of, but are not limited to, monoterpenes (β -myrcene, (E)- β -ocimene, terpinolene, limonene and β -pinene), alcohols (3-methyl-1-butanol, limited to pollen) and esters (hexenyl acetate). I set out to test which of these compounds may be detected by SIFT-MS.

4.3. Experimental Section

I adopted SIFT-MS methodology developed by Adams and Smith [3] as described in chapter 2 section 2.3. A detailed summary of SIFT-MS has previously been reported [75, 78, 83, 84, 86].

4.3.1. SIFT-MS Data Acquisition

SIFT-MS analysis was performed using a Profile 3 SIFT-MS spectrometer (Instrument Science, UK). I macerated the plant sample (average weight 1 to 3 grams) using a mortar and pestle, placed in a 250 mL beaker and immediately sealed with paraffin wax film. Using a needle attached to the SIFT nozzle, I pierced paraffin wax permitting sample intake over 5 minutes. Each sample triplicate was scanned 30 times at ten seconds per scan. I also analyzed laboratory air to allow me to subtract this background from actual sample mass spectra. Mass spectra are visual representations of the product ions generated by the SIFT-MS reaction. Plant sample spectra illustrate the product ions formed from the chemical ionization reactions that occur between the chosen precursor ion(s) and molecules emitted from the sample. Product ions within 10-300 m/z were detected. Results of the analyses are visualized as mass spectra. Analysis was repeated over two growing seasons, each of which yielded similar results.

4.3.2. SIFT-MS Data Handling and Display

Using the Mass Spectrometry Review (msview) software that accompanies the SIFT-MS instrument, I exported spectra from the SIFT-MS data system into Microsoft Excel, to complete calculations. An average of the product ions produced from each plant sample was calculated. The calculated values were then visualized as spectra for each sample (Figures 3 to 6). Major peaks were representative of the most abundant product ions produced. Thus, to ensure the spectra peaks were a true representation of a product ion rather than background noise, ion peaks with count per second (cps) greater than 40 were considered. Proposed products of the reactions between H_3O^+ and NO^+ with experimentally found compounds in *Polygala senega* [38], *Valeriana officinalis* [50]

and *Cannabis sativa* [67,68] were correlated with SIFT mass spectra of standard compounds for tentative identification (Tables 5 to 8).

4.4. Results and Discussion

SIFT-MS spectra for *Polygala senega*, *Valeriana officinalis* and *Cannabis sativa* (Figures 3 to 10) were generated using H_3O^+ and NO^+ precursor ions. O_2^+ was not used for analyses because many more fragment ions are formed with O_2^+ than with H_3O^+ and NO^+ as a result of the recombination energy of O_2^+ ions and thus, cannot be used as an effective means to determine parent compound structure [52 in 100, 87, 100]. Peaks illustrated in the spectra represent product ions and/or fragment ions produced by SIFT-MS analysis. High abundance chemical compounds may overwhelm the instrument by reacting away all the precursor ions creating the illusion that few product ions are being formed. For ease of presentation, plant spectra are shown in two parts at two different sensitivities a. m/z 1-100 and b. m/z 100-200 (note the variation in the scale of y-axis). The following tables (Tables 5 to 8) list compounds for which I have standard SIFT-MS signals and which were previously reported in *Polygala senega* [38], *Valeriana officinalis* [50] and *Cannabis sativa* [67, 68], respectively. Hayashi and Kameoka [38] extracted the essential oil component by steam distillation of dried *Polygala senega* roots followed by GC and GC-MS analysis. Similarly, Letchamo, Ward, Heard and Heard [50] extracted the essential oil component of *Valeriana officinalis* by hydro-distillation of dried roots followed by GC and GC-MS analysis. Likewise, Ross and ElSohly [67] extracted the essential oil of *Cannabis sativa* by air drying the plant material for various lengths of time from which the volatile oil was prepared by steam distillation followed by GC and GC-MS analysis. In contrast to the previous methods, Rothschild, Bergstrom and

Wangberg [68] collected head-space volatiles of *Cannabis sativa* in plastic bags. Air was extracted from the bags by micro pumps and volatiles were adsorbed from the air followed by solvent extraction [68]. The volatile samples were then analyzed by GC-MS [68]. The above research groups were able to identify compounds present in their respective plant samples by comparing experimental data with literature, reference standards and/or available databases [38, 50, 67, 68]. Many methods require samples to be extracted in liquid prior to volatilization and subsequent analysis. This process may affect the integrity of the chemical compounds by degrading their structure, which may in turn produce off flavours or aromas and lead to inaccurate interpretation of results [63]. In this report, I am analyzing the headspace of fresh plant material to determine if SIFT-MS can be utilized as a detection method of such compounds from *in vivo* samples without further manipulation of the sample. These compounds, or similar compounds, have been previously analyzed as standard compounds using SIFT-MS and the fragment ions produced are listed accordingly. The product ions identified by SIFT-MS analysis of plant emissions suggest which compounds may be present in the sample.

4.4.1. *Polygala senega* H_3O^+ Reactions

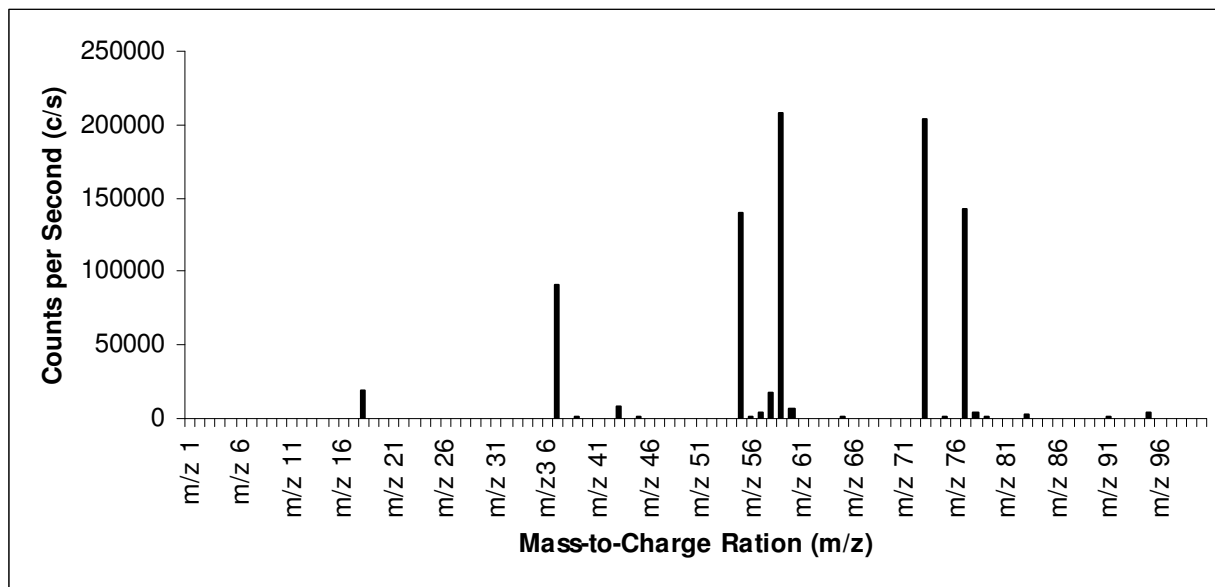
Generally, straight chain carboxylic acids produce two ions: 1. protonated parent compound ($R-COOH \cdot H^+$) and 2. hydroxide abstraction (R_1-CO^+), when reacted with H_3O^+ , where $R-COOH \cdot H^+$ is the major ion and subsequently R_1-CO^+ is the minor ion [87]. Typically, when the reaction yields both ions, the ions are present in a 9:1 ratio ($R-COOH \cdot H^+ : R_1-CO^+$) or $R-COOH \cdot H^+$ is the only ion formed [87]. Therefore, $R-COOH \cdot H^+$ and R_1-CO^+ must be identified in order to suggest that carboxylic acid is present in sufficient quantity to be detected. The above ions are present for hexanoic acid

in the typical ratio, as reported by Španěl and Smith [87], suggesting hexanoic acid is identifiable in the sample. These ions are not, however, detected for octanoic acid and nonanoic acid and therefore, cannot be identified in the *Polygala* H₃O⁺ SIFT spectra with certainty. Of the putative ions expected from the reactions of valeric acid with H₃O⁺ (*m/z* 85 and 103), *m/z* 103 is detected in the spectra and further analysis is required to determine if valeric acid is actually present in this sample (Fig. 3b). Salicylic acid, on the other hand, is a cyclical carboxylic acid with an additional hydroxide constituent. This type of compound has been shown to undergo hydroxide ion abstraction, which is the major fragmentation route, and produce the minor compound R-COOH·H⁺ [87]. Salicylic acid conforms to this pattern and produces C₇H₆O₃·H⁺ (*m/z* 139) and C₇H₅O₂⁺ (*m/z* 121) which are tentatively identified in the *Polygala senega* SIFT spectra (Fig. 3b); however cps for *m/z* 139 is low. This pattern is also seen for heptanoic acid which produces C₆H₁₃COOH·H⁺ (*m/z* 131) and C₆H₁₃CO⁺ (*m/z* 113). The ion peak at *m/z* 113 is seen in the spectra (Fig. 3b). Since hydroxide ion abstraction is typically observed for carboxylic acids with an additional hydroxide group [87], ion peak *m/z* 113 cannot be used as an indicator for heptanoic acid.

Characteristic ion peaks are produced for hexanal (R₁-CHO·H⁺ and R₁-C⁺). Španěl and Smith [85] report an equal production of each ion, while the *Polygala senega* spectra show a significantly greater abundance of the hydroxide abstraction reaction process. Additional analysis is needed to conclude if peaks *m/z* 83 (2699 cps, Fig. 3a) and *m/z* 101 (103 cps, Fig 3b), represent hexanal.

The protonated parent compound is the sole ion produced for *o*-cresol [101]. Ion

a.



b.

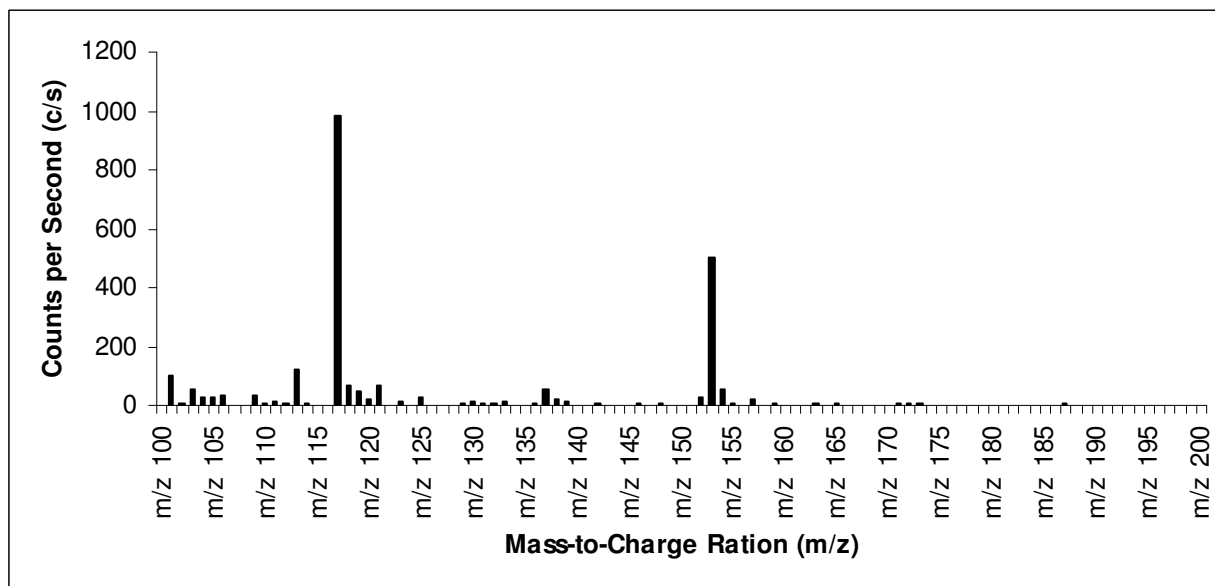
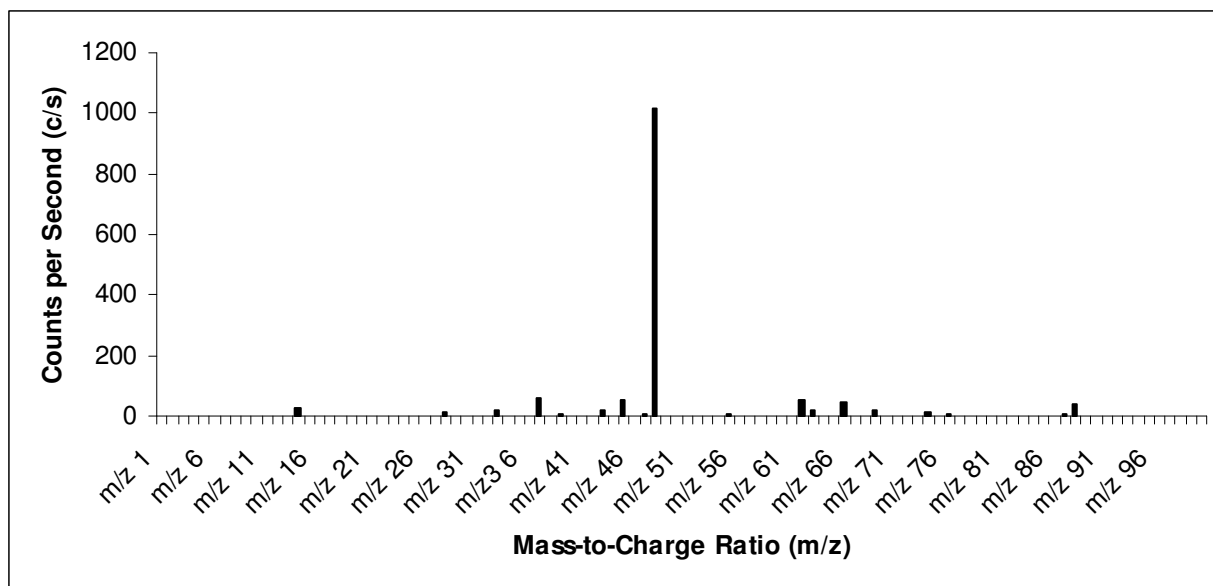


Figure 3. Analysis of *Polygala senega*; mass spectra generated with H_3O^+ . a. m/z 1-100; b. m/z 100-200. (Note different scales of the y-axis).

a.



b.

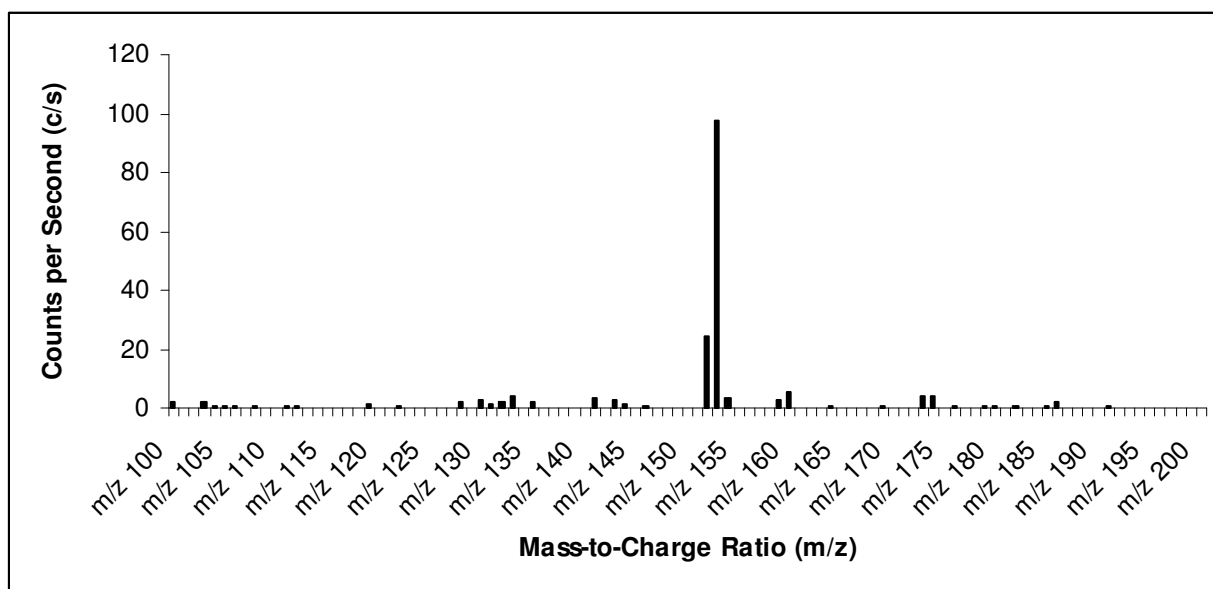
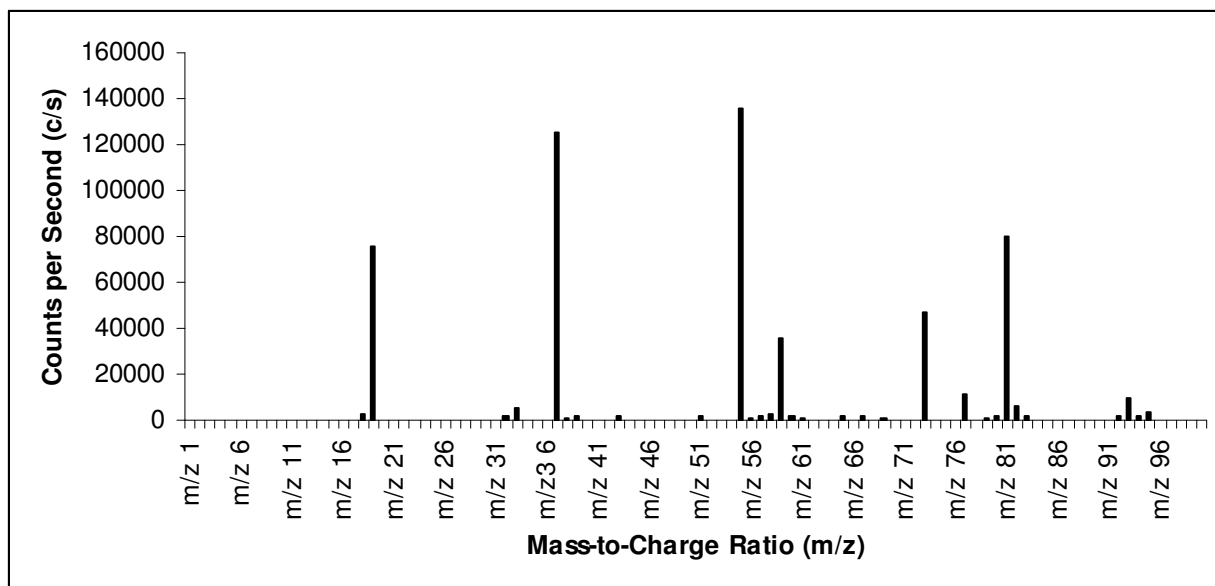


Figure 4. Analysis of *Polygala senega*; mass spectra generated with NO^+ . a. m/z 1-100; b. m/z 100-200.

a.



b.

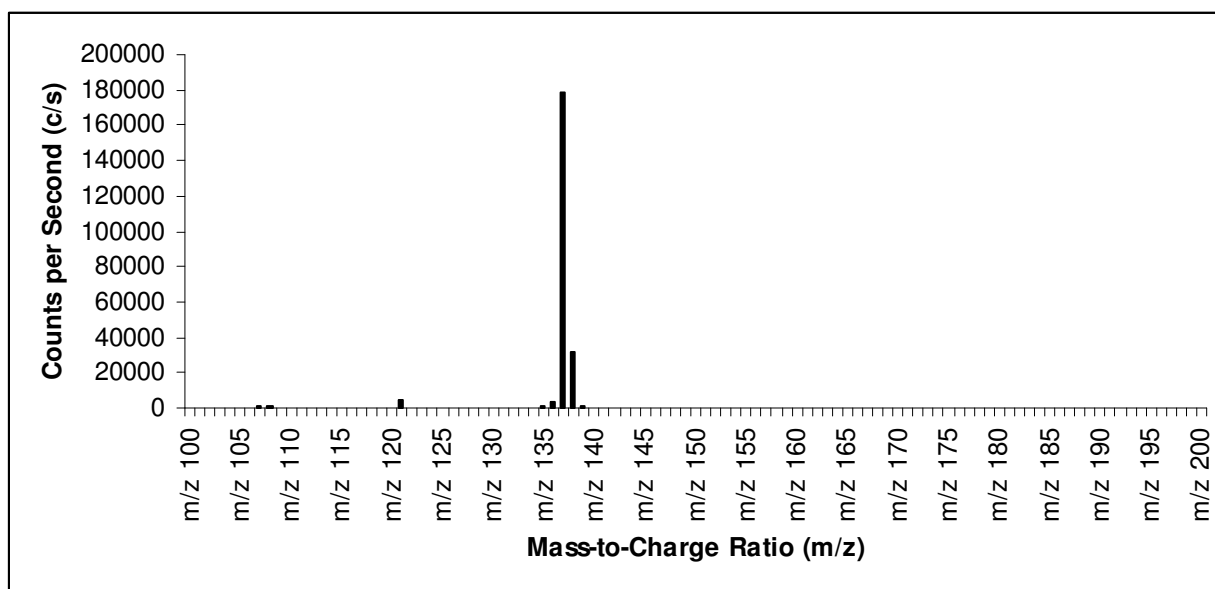
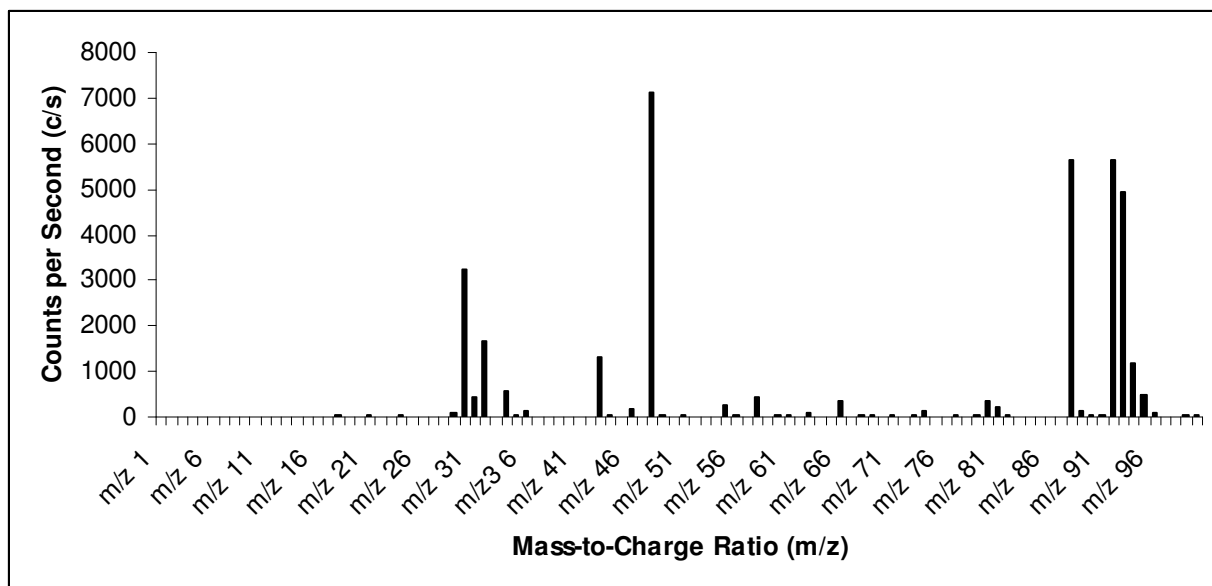


Figure 5. Analysis of *Valeriana officinalis*; mass spectra generated with H_3O^+ . a. m/z 1-100; b. m/z 100-200.

a.



b.

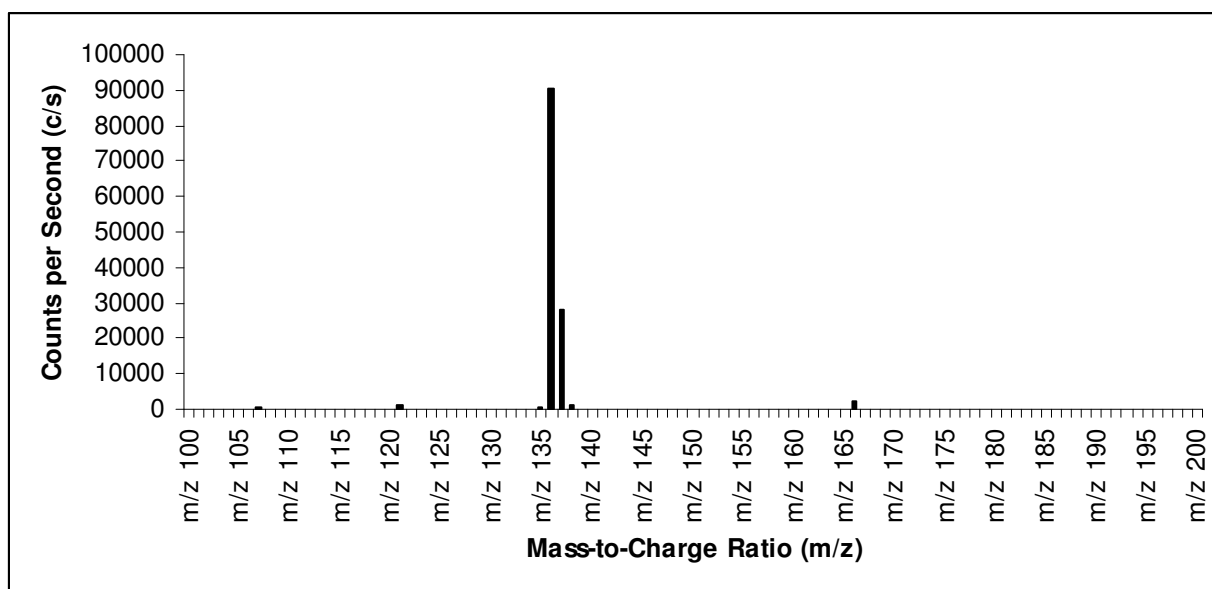
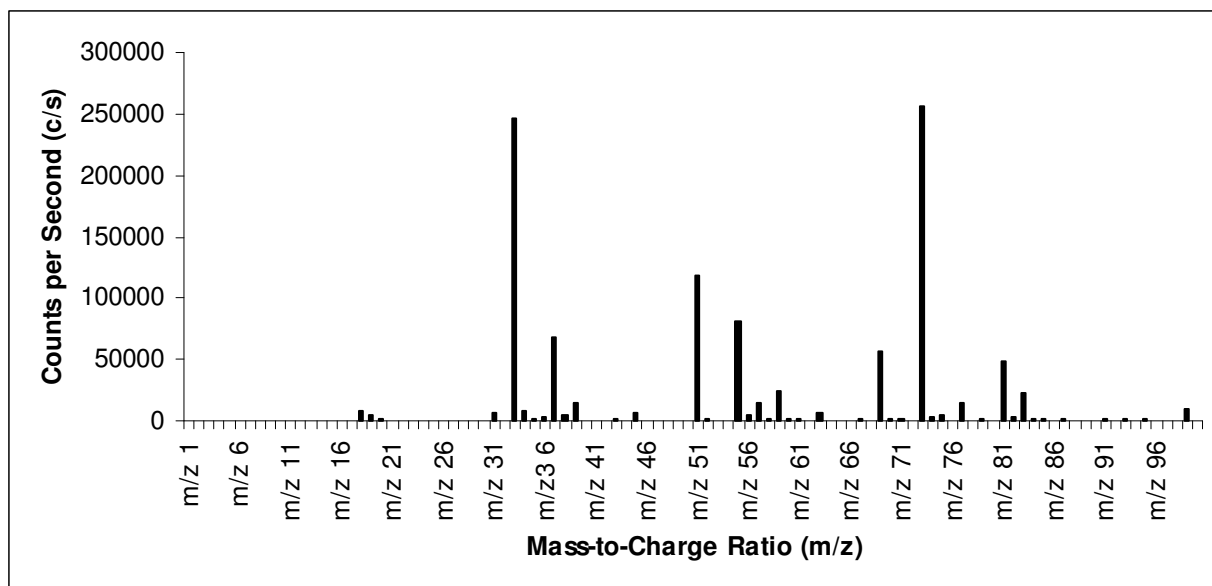


Figure 6. Analysis of *Valeriana officinalis*; mass spectra generated with NO^+ . a. m/z 1-100; b. m/z 100-200.

a.



b.

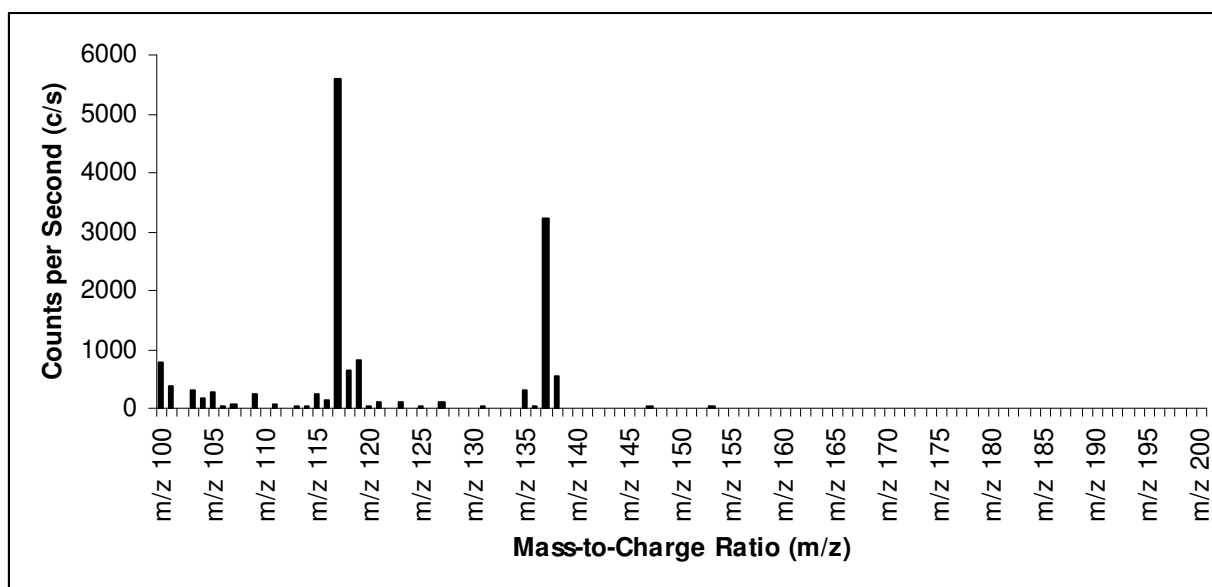
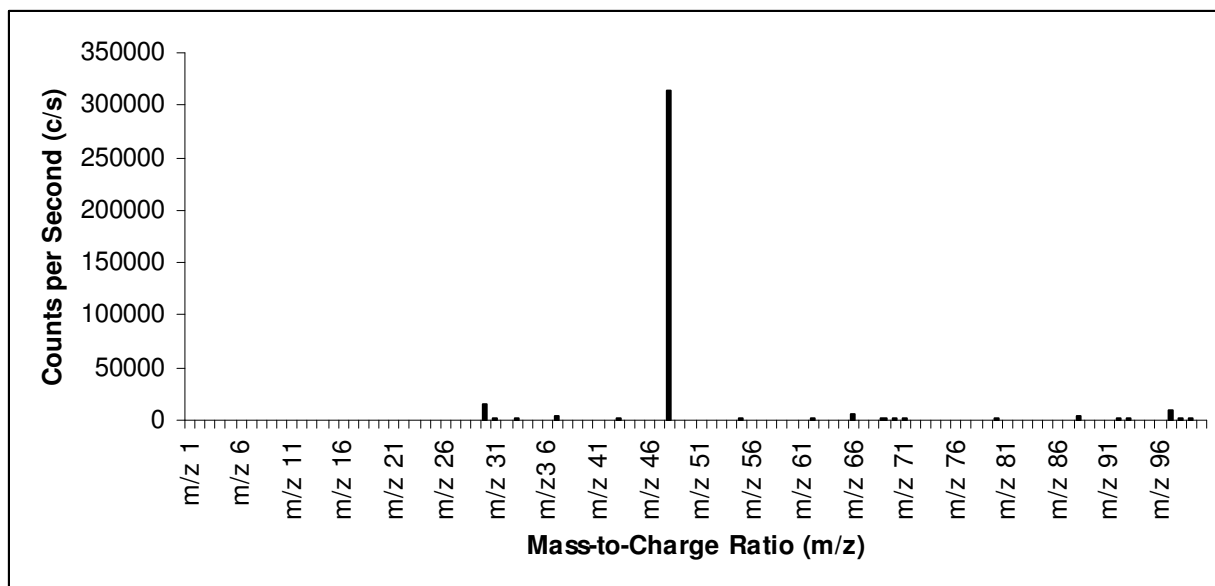


Figure 7. Analysis of *Cannabis sativa* leaves; mass spectra generated with H_3O^+ . a. m/z 1-100; b. m/z 100-200.

a.



b.

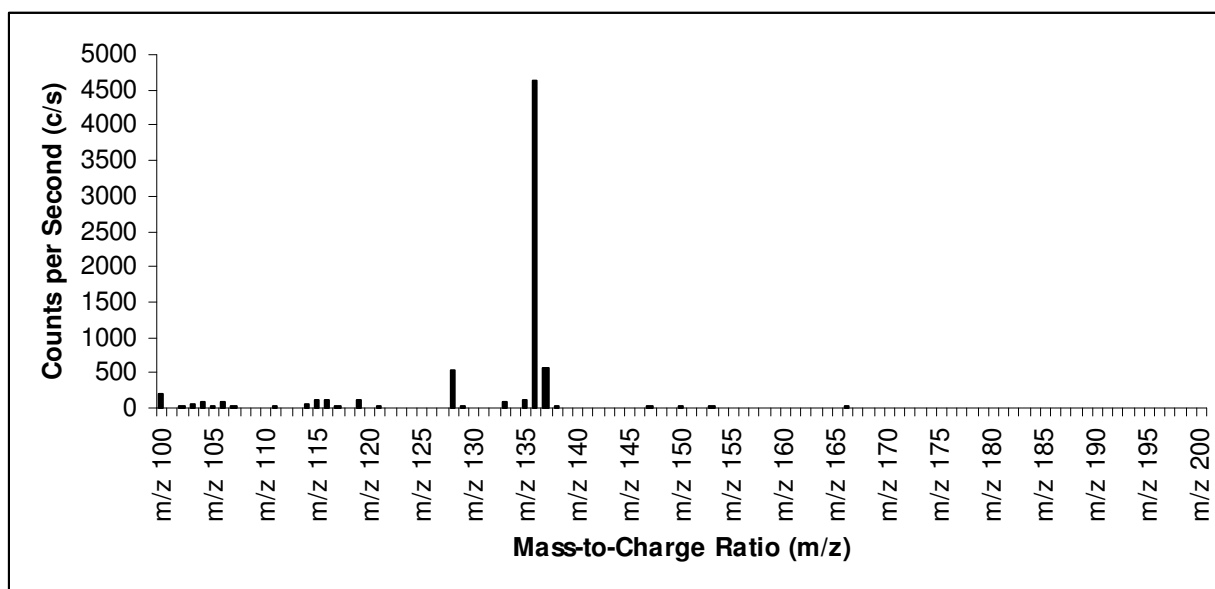
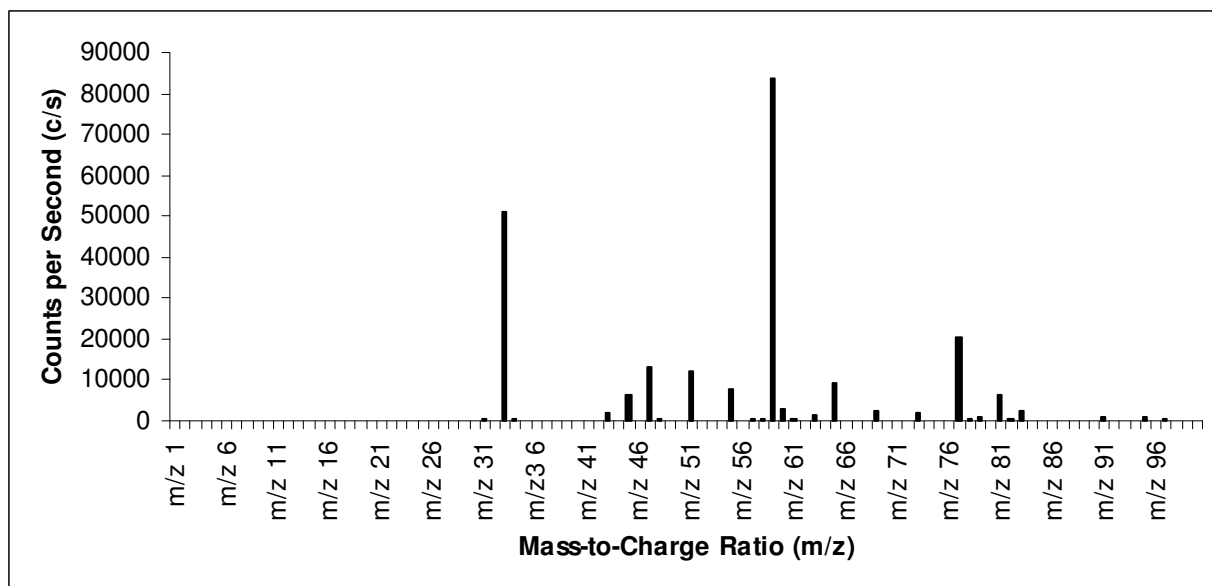


Figure 8. Analysis of *Cannabis sativa* leaves; mass spectra generated with NO^+ . a. m/z 1-100; b. m/z 100-200.

a.



b.

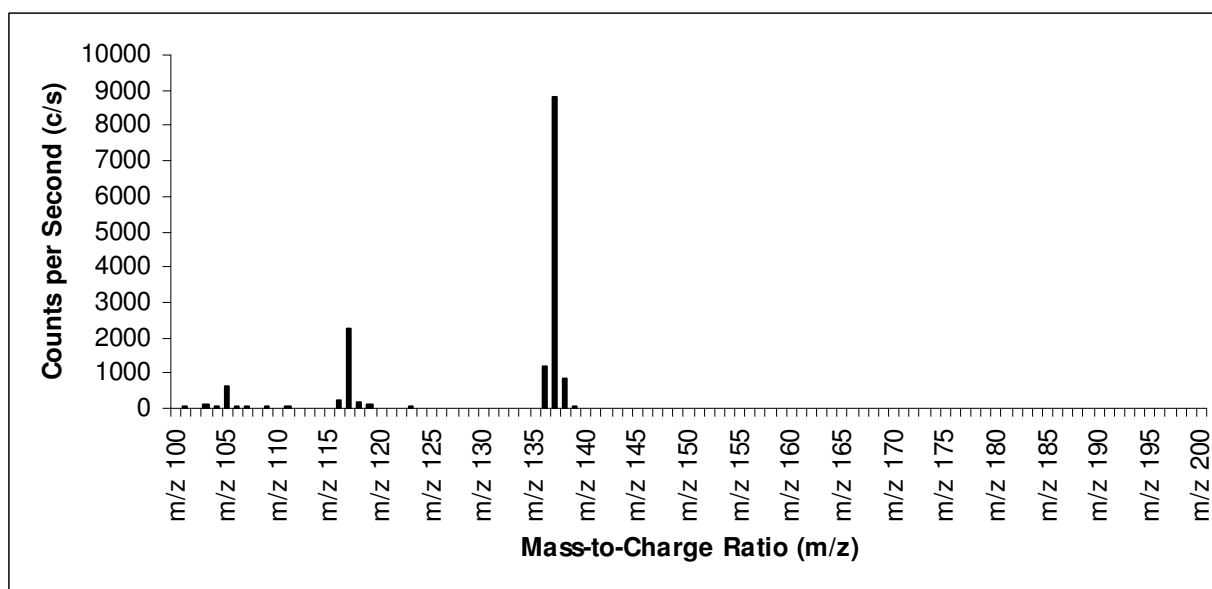
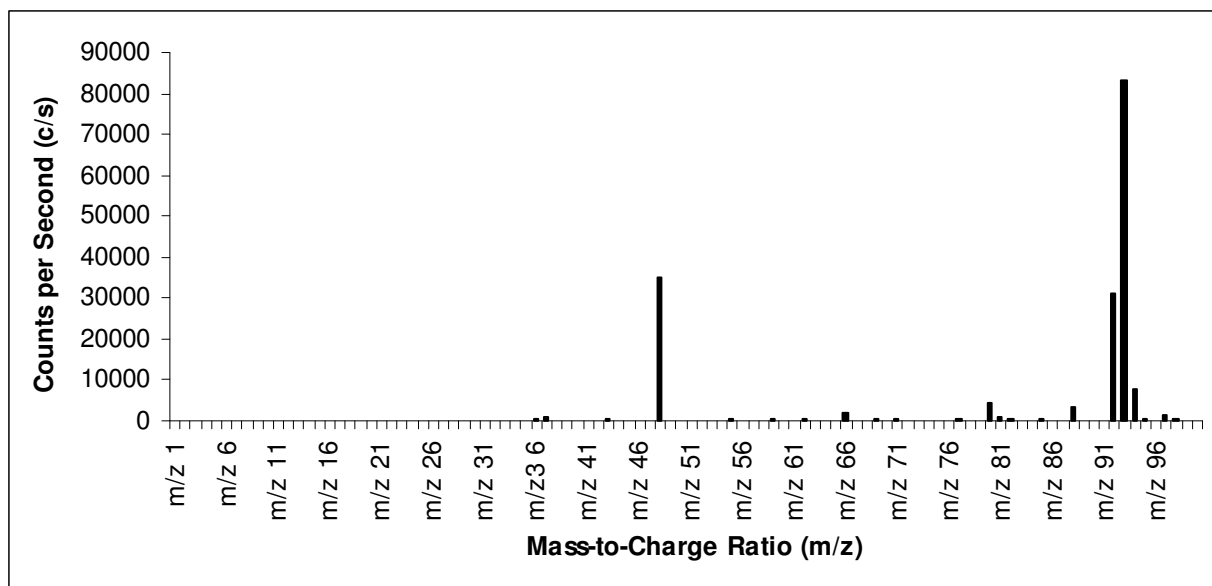


Figure 9. Analysis of *Cannabis sativa* seeds; mass spectra generated with H_3O^+ . a. m/z 1-100; b. m/z 100-200.

a.



b.

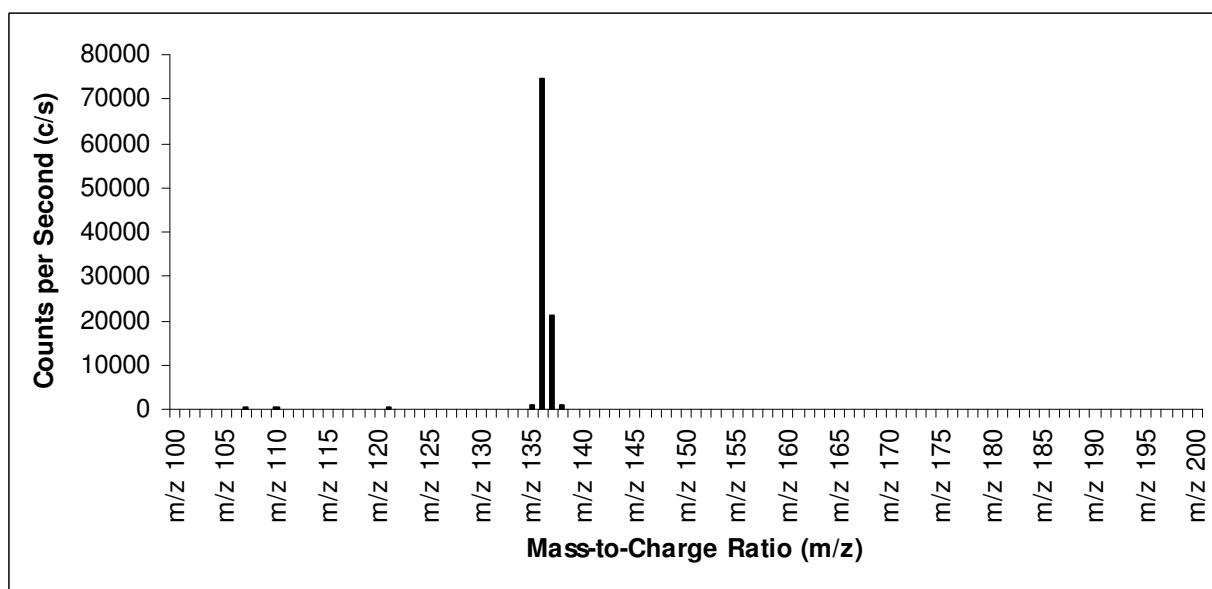


Figure 10. Analysis of *Cannabis sativa* seeds; mass spectra generated with NO^+ . a. m/z 1-100; b. m/z 100-200.

Table 5. Putative products of the reactions between H_3O^+ and NO^+ with previously analyzed standard compounds in *Polygala senega* [38]. These compounds, or similar compounds, have been previously analyzed using SIFT-MS [85, 87, 100]. The molecular formulae of the ion products given may not be an exact representation of their structure. Product ions with at least 40 cps that can be correlated to my SIFT-MS analysis of *Polygala senega* are illustrated in bold font.

| Compound | H_3O^+ | NO^+ |
|--|---|---|
| valeric acid $\text{C}_4\text{H}_9\text{COOH}$ | $\text{C}_4\text{H}_9\text{CO}^+ + 2\text{H}_2\text{O}$ (<i>m/z</i> 85) $\text{C}_4\text{H}_9\text{COOH}\cdot\text{H}^+$ + H_2O (<i>m/z</i> 103) | $\text{C}_4\text{H}_9\text{CO}^+ + \text{HNO}_2$ (<i>m/z</i> 85) $\text{C}_4\text{H}_9\text{COOH}\cdot\text{NO}^+$ (<i>m/z</i> 132) |
| hexanoic acid $\text{C}_5\text{H}_{11}\text{COOH}$ | $\text{C}_5\text{H}_{11}\text{CO}^+$ + $2\text{H}_2\text{O}$ (<i>m/z</i> 99) $\text{C}_5\text{H}_{11}\text{COOH}\cdot\text{H}^+$ + H_2O (<i>m/z</i> 117) | $\text{C}_5\text{H}_{11}\text{CO}^+ + \text{HNO}_2$ (<i>m/z</i> 99) $\text{C}_5\text{H}_{11}\text{COOH}\cdot\text{NO}^+$ (<i>m/z</i> 146) |
| heptanoic acid $\text{C}_6\text{H}_{13}\text{COOH}$ | $\text{C}_6\text{H}_{13}\text{CO}^+$ + $2\text{H}_2\text{O}$ (<i>m/z</i> 113) $\text{C}_6\text{H}_{13}\text{COOH}\cdot\text{H}^+$ + H_2O (<i>m/z</i> 131) | $\text{C}_6\text{H}_{13}\text{CO}^+ + \text{HNO}_2$ (<i>m/z</i> 113) $\text{C}_6\text{H}_{13}\text{COOH}\cdot\text{NO}^+$ (<i>m/z</i> 160) |
| octanoic acid $\text{C}_7\text{H}_{15}\text{COOH}$ | $\text{C}_7\text{H}_{15}\text{CO}^+ + 2\text{H}_2\text{O}$ (<i>m/z</i> 127) $\text{C}_7\text{H}_{15}\text{COOH}\cdot\text{H}^+$ + H_2O (<i>m/z</i> 145) | $\text{C}_7\text{H}_{15}\text{CO}^+ + \text{HNO}_2$ (<i>m/z</i> 127) $\text{C}_7\text{H}_{15}\text{COOH}\cdot\text{NO}^+$ (<i>m/z</i> 174) |
| nonanoic acid $\text{C}_8\text{H}_{17}\text{COOH}$ | $\text{C}_8\text{H}_{17}\text{CO}^+ + 2\text{H}_2\text{O}$ (<i>m/z</i> 141) $\text{C}_8\text{H}_{17}\text{COOH}\cdot\text{H}^+$ + H_2O (<i>m/z</i> 159) | $\text{C}_8\text{H}_{17}\text{CO}^+ + \text{HNO}_2$ (<i>m/z</i> 141) $\text{C}_8\text{H}_{17}\text{COOH}\cdot\text{NO}^+$ (<i>m/z</i> 188) |
| salicylic acid $\text{C}_6\text{H}_6\text{CO}_3$ | $\text{C}_7\text{H}_5\text{O}_2^+$ + $2\text{H}_2\text{O}$ (<i>m/z</i> 121) $\text{C}_7\text{H}_6\text{O}_3\cdot\text{H}^+$ + H_2O (<i>m/z</i> 139) | $\text{C}_7\text{H}_5\text{O}_2^+ + \text{HNO}_2$ (<i>m/z</i> 121) $\text{C}_7\text{H}_6\text{O}_3\cdot\text{NO}^+$ (<i>m/z</i> 168) |
| hexanal $\text{C}_5\text{H}_{11}\text{CHO}$ | $\text{C}_5\text{H}_{11}\text{C}^+$ + $2\text{H}_2\text{O}$ (<i>m/z</i> 83) $\text{C}_5\text{H}_{11}\text{CHO}\cdot\text{H}^+$ + $2\text{H}_2\text{O}$ (<i>m/z</i> 101) | $\text{C}_5\text{H}_{11}\text{CO}^+ + \text{HNO}$ (<i>m/z</i> 99) |
| <i>o</i> -Cresol $\text{C}_7\text{H}_8\text{O}$ | $\text{C}_7\text{H}_8\text{O}\cdot\text{H}^+$ + H_2O (<i>m/z</i> 109) | $\text{C}_7\text{H}_8\text{O}^+ + \text{NO}$ (<i>m/z</i> 138) |
| methyl salicylate $\text{C}_8\text{H}_8\text{O}_3$ | $\text{C}_8\text{H}_8\text{O}_3\cdot\text{H}^+$ + H_2O (<i>m/z</i> 153) | $\text{C}_8\text{H}_8\text{O}_3\cdot\text{NO}^+$ (<i>m/z</i> 182) |

Table 6. Putative products of the reactions between H_3O^+ and NO^+ with experimentally found compounds in *Valeriana officinalis* [50]. Product/fragment ions for these reactions are assumed based on previously published work of similar compounds analyzed using SIFT-MS [85, 87, 100]. The molecular formulae of the ion products given may not be an exact representation of their structure. Product ions with at least 40 cps that can be correlated to my SIFT-MS analysis of *Valeriana officinalis* are illustrated in bold font.

| Compound | H_3O^+ | NO^+ |
|---|---|---|
| camphene $\text{C}_{10}\text{H}_{16}$ | C_6H_9^+ + $\text{C}_4\text{H}_7\cdot\text{H}$ + H_2O (m/z 81) $\text{C}_{10}\text{H}_{16}\cdot\text{H}^+$ + H_2O (m/z 137) | C_7H_8^+ + $\text{C}_3\text{H}_8\cdot\text{NO}$ (m/z 92) C_7H_9^+ + $\text{C}_3\text{H}_7\cdot\text{NO}$ (m/z 93) $\text{C}_{10}\text{H}_{16}^+$ + NO (m/z 136) |
| bornyl acetate $\text{C}_{12}\text{H}_{20}\text{O}_2$ | $\text{C}_{10}\text{H}_{17}^+$ + $\text{C}_2\text{H}_3\text{O}_2\cdot\text{H}$ + H_2O (m/z 137) $\text{C}_{11}\text{H}_{17}\text{O}_2^+$ + $\text{CH}_3\cdot\text{H}$ + H_2O (m/z 181) $\text{C}_{12}\text{H}_{20}\text{O}_2\cdot\text{H}^+$ + H_2O (m/z 197) | $\text{C}_{10}\text{H}_{17}^+$ + $\text{C}_2\text{H}_3\cdot\text{NO}_3$ (m/z 137) $\text{C}_{11}\text{H}_{17}\text{O}_2^+$ + $\text{CH}_3\cdot\text{NO}$ (m/z 181) $\text{C}_{12}\text{H}_{20}\text{O}_2\cdot\text{NO}^+$ (m/z 226) |
| valerenal $\text{C}_{15}\text{H}_{22}\text{O}$ | $\text{C}_{11}\text{H}_{17}^+$ + $\text{C}_4\text{H}_5\text{O}^+$ + H_2O (m/z 149) $\text{C}_{15}\text{H}_{21}^+$ + $2\text{H}_2\text{O}$ (m/z 201) $\text{C}_{15}\text{H}_{22}\text{O}\cdot\text{H}^+$ + H_2O (m/z 219) | $\text{C}_{11}\text{H}_{17}^+$ + $\text{C}_4\text{H}_5\cdot\text{NO}$ (m/z 149) $\text{C}_{15}\text{H}_{21}\text{O}^+$ + HNO (m/z 217) $\text{C}_{15}\text{H}_{22}\text{O}\cdot\text{NO}$ (m/z 248) |
| valerenic acid $\text{C}_{15}\text{H}_{22}\text{O}_2$ | $\text{C}_{15}\text{H}_{21}\text{O}^+$ + $2\text{H}_2\text{O}$ (m/z 217) $\text{C}_{15}\text{H}_{22}\text{O}_2\cdot\text{H}^+$ + H_2O (m/z 235) | $\text{C}_{15}\text{H}_{21}\text{O}_2^+$ + HNO (m/z 233) $\text{C}_{15}\text{H}_{22}\text{O}_2\cdot\text{NO}^+$ (m/z 264) |
| 15-acetoxy valeranone $\text{C}_{17}\text{H}_{28}\text{O}_4$ | $\text{C}_{16}\text{H}_{25}\text{O}_3^+$ + $\text{CH}_3\text{O}\cdot\text{H}$ + H_2O (m/z 265) $\text{C}_{17}\text{H}_{28}\text{O}_4\cdot\text{H}^+$ + H_2O (m/z 297) | $\text{C}_{16}\text{H}_{25}\text{O}_3^+$ + CH_3NO_2 (m/z 265) $\text{C}_{17}\text{H}_{28}\text{O}_4^+$ + NO (m/z 296) $\text{C}_{17}\text{H}_{28}\text{O}_4\cdot\text{NO}^+$ (m/z 326)* |

*exceeds chosen m/z rang for analyses

Table 7. Putative products of the reactions between H_3O^+ and NO^+ with experimentally found compounds in *Cannabis sativa* leaves [67, 68]. These compounds, or similar compounds, have been previously analyzed using SIFT-MS [4, 86, 100]. The molecular formulae of the ion products given may not be an exact representation of their structure. Product ions with at least 40 cps that can be correlated to my SIFT-MS analysis of *Cannabis sativa* leaves are illustrated in bold font.

| Compound | H_3O^+ | NO^+ |
|---|---|---|
| Myrcene $\text{C}_{10}\text{H}_{16}$ | C_5H_9^+ + $\text{C}_5\text{H}_7\cdot\text{H}$ + H_2O (m/z 69) C_6H_9^+ + $\text{C}_4\text{H}_7\cdot\text{H}$ + H_2O (m/z 81) $\text{C}_7\text{H}_{11}^+$ + $\text{C}_3\text{H}_5\cdot\text{H}$ + H_2O (m/z 95) $\text{C}_{10}\text{H}_{16}\cdot\text{H}^+$ + H_2O (m/z 137) | C_7H_8^+ + $\text{C}_3\text{H}_8\cdot\text{NO}$ (m/z 92) C_7H_9^+ + $\text{C}_3\text{H}_7\cdot\text{NO}$ (m/z 93) $\text{C}_{10}\text{H}_{16}^+$ + NO (m/z 136) |
| Ocimene $\text{C}_{10}\text{H}_{16}$ | C_4H_9^+ + $\text{C}_6\text{H}_7\cdot\text{H}$ + H_2O (m/z 57) C_5H_9^+ + $\text{C}_5\text{H}_7\cdot\text{H}$ + H_2O (m/z 69) C_6H_9^+ + $\text{C}_4\text{H}_7\cdot\text{H}$ + H_2O (m/z 81) $\text{C}_7\text{H}_{11}^+$ + $\text{C}_3\text{H}_5\cdot\text{H}$ + H_2O (m/z 95) $\text{C}_{10}\text{H}_{16}\cdot\text{H}^+$ + H_2O (m/z 137) | C_7H_8^+ + $\text{C}_3\text{H}_8\cdot\text{NO}$ (m/z 92) C_7H_9^+ + $\text{C}_3\text{H}_7\cdot\text{NO}$ (m/z 93) $\text{C}_{10}\text{H}_{16}^+$ + NO (m/z 136) |
| Terpinolene $\text{C}_{10}\text{H}_{16}$ | C_6H_9^+ + $\text{C}_4\text{H}_7\cdot\text{H}$ + H_2O (m/z 81) $\text{C}_{10}\text{H}_{15}^+$ + H_2 + H_2O (m/z 135) $\text{C}_{10}\text{H}_{16}\cdot\text{H}^+$ + H_2O (m/z 137) | C_7H_8^+ + $\text{C}_3\text{H}_8\cdot\text{NO}$ (m/z 92) C_7H_9^+ + $\text{C}_3\text{H}_7\cdot\text{NO}$ (m/z 93) $\text{C}_{10}\text{H}_{15}^+$ + HNO (m/z 135) $\text{C}_{10}\text{H}_{16}^+$ + NO (m/z 136) |
| β -Pinene $\text{C}_{10}\text{H}_{16}$ | C_6H_9^+ + $\text{C}_4\text{H}_7\cdot\text{H}$ + H_2O (m/z 81) $\text{C}_{10}\text{H}_{16}\cdot\text{H}^+$ + H_2O (m/z 137) | C_7H_8^+ + $\text{C}_3\text{H}_8\cdot\text{NO}$ (m/z 92) C_7H_9^+ + $\text{C}_3\text{H}_7\cdot\text{NO}$ (m/z 93) $\text{C}_{10}\text{H}_{16}^+$ + NO (m/z 136) |
| Limonene $\text{C}_{10}\text{H}_{16}$ | C_6H_9^+ + $\text{C}_4\text{H}_7\cdot\text{H}$ + H_2O (m/z 81) $\text{C}_7\text{H}_{11}^+$ + $\text{C}_3\text{H}_5\cdot\text{H}$ + H_2O (m/z 95) $\text{C}_{10}\text{H}_{16}\cdot\text{H}^+$ + H_2O (m/z 137) | C_7H_8^+ + $\text{C}_3\text{H}_8\cdot\text{NO}$ (m/z 92) C_7H_9^+ + $\text{C}_3\text{H}_7\cdot\text{NO}$ (m/z 93) $\text{C}_7\text{H}_{10}^+$ + $\text{C}_3\text{H}_6\cdot\text{NO}$ (m/z 94) $\text{C}_9\text{H}_{13}^+$ + $\text{CH}_3\cdot\text{NO}$ (m/z 121) $\text{C}_{10}\text{H}_{15}^+$ + HNO (m/z 135) $\text{C}_{10}\text{H}_{16}^+$ + NO (m/z 136) |
| 3-methyl-1-butanol $\text{C}_5\text{H}_{11}\text{O}$ | $\text{C}_5\text{H}_{11}^+$ + $2\text{H}_2\text{O}$ (m/z 71) | $\text{C}_5\text{H}_{11}^+$ + 2NO_2 (m/z 71) $\text{C}_5\text{H}_{11}\text{O}^+$ + NO (m/z 87) |
| Linalool $\text{C}_{10}\text{H}_{18}\text{O}$ | C_6H_9^+ + $\text{C}_4\text{H}_7\cdot\text{H}$ + H_2O (m/z 81) $\text{C}_{10}\text{H}_{17}^+$ + $2\text{H}_2\text{O}$ (m/z 137) | $\text{C}_{10}\text{H}_{16}^+$ + NO (m/z 136) $\text{C}_{10}\text{H}_{18}\text{O}^+$ + NO (m/z 154) |

Table 8. Putative products of the reactions between H_3O^+ and NO^+ with experimentally found compounds in *Cannabis sativa* seeds [67, 68]. These compounds, or similar compounds, have been previously analyzed using SIFT-MS [4, 86, 100]. The molecular formulae of the ion products given may not be an exact representation of their structure. Product ions with at least 40 cps that can be correlated to my SIFT-MS analysis of *Cannabis sativa* seeds are illustrated in bold font.

| Compound | H_3O^+ | NO^+ |
|---|---|---|
| Myrcene $\text{C}_{10}\text{H}_{16}$ | C_5H_9^+ + $\text{C}_3\text{H}_7\cdot\text{H}$ + H_2O (m/z 69) C_6H_9^+ + $\text{C}_4\text{H}_7\cdot\text{H}$ + H_2O (m/z 81) $\text{C}_7\text{H}_{11}^+$ + $\text{C}_3\text{H}_5\cdot\text{H}$ + H_2O (m/z 95) $\text{C}_{10}\text{H}_{16}\cdot\text{H}^+$ + H_2O (m/z 137) | C_7H_8^+ + $\text{C}_3\text{H}_8\cdot\text{NO}$ (m/z 92) C_7H_9^+ + $\text{C}_3\text{H}_7\cdot\text{NO}$ (m/z 93) $\text{C}_{10}\text{H}_{16}^+$ + NO (m/z 136) |
| Ocimene $\text{C}_{10}\text{H}_{16}$ | C_4H_9^+ + $\text{C}_6\text{H}_7\cdot\text{H}$ + H_2O (m/z 57) C_5H_9^+ + $\text{C}_3\text{H}_7\cdot\text{H}$ + H_2O (m/z 69) C_6H_9^+ + $\text{C}_4\text{H}_7\cdot\text{H}$ + H_2O (m/z 81) $\text{C}_7\text{H}_{11}^+$ + $\text{C}_3\text{H}_5\cdot\text{H}$ + H_2O (m/z 95) $\text{C}_{10}\text{H}_{16}\cdot\text{H}^+$ + H_2O (m/z 137) | C_7H_8^+ + $\text{C}_3\text{H}_8\cdot\text{NO}$ (m/z 92) C_7H_9^+ + $\text{C}_3\text{H}_7\cdot\text{NO}$ (m/z 93) $\text{C}_{10}\text{H}_{16}^+$ + NO (m/z 136) |
| Terpinolene $\text{C}_{10}\text{H}_{16}$ | C_6H_9^+ + $\text{C}_4\text{H}_7\cdot\text{H}$ + H_2O (m/z 81) $\text{C}_{10}\text{H}_{15}^+$ + H_2 + H_2O (m/z 135) $\text{C}_{10}\text{H}_{16}\cdot\text{H}^+$ + H_2O (m/z 137) | C_7H_8^+ + $\text{C}_3\text{H}_8\cdot\text{NO}$ (m/z 92) C_7H_9^+ + $\text{C}_3\text{H}_7\cdot\text{NO}$ (m/z 93) $\text{C}_{10}\text{H}_{15}^+$ + HNO (m/z 135) $\text{C}_{10}\text{H}_{16}^+$ + NO (m/z 136) |
| β -Pinene $\text{C}_{10}\text{H}_{16}$ | C_6H_9^+ + $\text{C}_4\text{H}_7\cdot\text{H}$ + H_2O (m/z 81) $\text{C}_{10}\text{H}_{16}\cdot\text{H}^+$ + H_2O (m/z 137) | C_7H_8^+ + $\text{C}_3\text{H}_8\cdot\text{NO}$ (m/z 92) C_7H_9^+ + $\text{C}_3\text{H}_7\cdot\text{NO}$ (m/z 93) $\text{C}_{10}\text{H}_{16}^+$ + NO (m/z 136) |
| Limonene $\text{C}_{10}\text{H}_{16}$ | C_6H_9^+ + $\text{C}_4\text{H}_7\cdot\text{H}$ + H_2O (m/z 81) $\text{C}_7\text{H}_{11}^+$ + $\text{C}_3\text{H}_5\cdot\text{H}$ + H_2O (m/z 95) $\text{C}_{10}\text{H}_{16}\cdot\text{H}^+$ + H_2O (m/z 137) | C_7H_8^+ + $\text{C}_3\text{H}_8\cdot\text{NO}$ (m/z 92) C_7H_9^+ + $\text{C}_3\text{H}_7\cdot\text{NO}$ (m/z 93) $\text{C}_7\text{H}_{10}^+$ + $\text{C}_3\text{H}_6\cdot\text{NO}$ (m/z 94) $\text{C}_9\text{H}_{13}^+$ + $\text{CH}_3\cdot\text{NO}$ (m/z 121) $\text{C}_{10}\text{H}_{15}^+$ + HNO (m/z 135) $\text{C}_{10}\text{H}_{16}^+$ + NO (m/z 136) |
| 3-methyl-1-butanol $\text{C}_5\text{H}_{11}\text{O}$ | $\text{C}_5\text{H}_{11}^+$ + $2\text{H}_2\text{O}$ (m/z 71) | $\text{C}_5\text{H}_{11}^+$ + 2NO_2 (m/z 71) $\text{C}_5\text{H}_{11}\text{O}^+$ + NO (m/z 87) |
| Linalool $\text{C}_{10}\text{H}_{18}\text{O}$ | C_6H_9^+ + $\text{C}_4\text{H}_7\cdot\text{H}$ + H_2O (m/z 81) $\text{C}_{10}\text{H}_{17}^+$ + $2\text{H}_2\text{O}$ (m/z 137) | $\text{C}_{10}\text{H}_{16}^+$ + NO (m/z 136) $\text{C}_{10}\text{H}_{18}\text{O}^+$ + NO (m/z 154) |

peak m/z 109 is a potential representative of the protonated *o*-cresol; however, this peak cannot be used as an indication of *o*-cresol detection because of low cps (Fig. 3b) and further analysis is required.

The protonated parent compound is the sole ion produced with methyl salicylate in great quantity (Table 4). This peak (m/z 153, Fig. 3b) is clearly detected as an ion peak in the spectra and very likely represents methyl salicylate. This conclusion is further corroborated by Hayashi and Kameoka [38] who found that methyl salicylate is an abundant compound in the plant material. In cases where spectra reveal enough information to suspect but not confirm that a particular compound has been identified, then the sample may be further analysed with a second precursor ion, NO^+ .

4.4.2. *Polygala senega* NO^+ Reactions

In contrast to H_3O^+ reactions, carboxylic acid- NO^+ reactions commonly result in the formation of an adduct ion ($\text{R}_1\text{-CHO}\cdot\text{NO}^+$) and hydroxide abstraction [87]. As found with the H_3O^+ reactions, heptanoic acid, octanoic acid and nonanoic acid cannot be identified in the plant sample with confidence using SIFT-MS. Also ion peaks representative of the ions resulting from the reactions of valeric acid and hexanoic acid with NO^+ cannot be used to identify these compounds in the spectra (Fig. 4). Any peaks that may be visible in the spectra (m/z 146 hexanoic acid, m/z 160 heptanoic acid, m/z 174 octanoic acid and m/z 141 nonanoic acid) (Fig. 4b) have a cps of less than 40 and cannot be assumed to be a true representation of the compound.

The detection of salicylic acid seems promising and likely using the H_3O^+ spectra; however, analysis with NO^+ cannot confirm this. Salicylic acid produces a single ion, deprotonated parent compound of m/z 182, which is not seen in (Fig. 4b).

The m/z 99 ion is likely indicative of the deprotonated parent compound hexanal. This peak has a cps of 75.9 which is sufficient to be seen as a peak on the spectra; however, this peak is not seen in the spectra (Fig. 4a). In combination with the results from H_3O^+ reactions, additional analysis is required to confirm that the product ion peaks represent hexanal.

Adduct ions are the standard ions formed from the phenol- NO^+ reaction [101]. In the case of *o*-cresol, this adduct ion is not detected. As a result, the presence of *o*-cresol in *Polygala senega* cannot be currently confirmed by SIFT-MS.

Similar to *o*-cresol, the adduct ion is the sole ion expected from reaction with NO^+ and methyl salicylate (Table 4). Methyl salicylate is one of the most abundant compounds in *Polygala senega* [38]. The ion with m/z 182 is not detected, which may be due to lack of volatility. NO^+ cannot be used to confirm that methyl salicylate has been detected in the sample of *Polygala senega*.

4.4.3. *Valeriana officinalis* H_3O^+ and NO^+ Reactions

Majority of the abundant constituents in *Valeriana officinalis*, as reported by Letchamo, Ward and Heard and Heard [50], have a high molecular weight. This posed a problem for SIFT-MS analysis, where typically lower molecular weight compounds are detectable. For many of the compounds, few characteristic peaks were visualized on the mass spectra, however, the peaks which represent higher molecular weight product/fragment ions could not be detected, most likely due to lack of volatility. The proportion of the product/fragment ions formed by the interaction with H_3O^+ and NO^+ with the plant compounds are used to determine if the molecule is identifiable in the spectra. Therefore, the distinctive compounds which are unique to *Valeriana officinalis*

[50] could not be identified and another means of analysis, perhaps a method which does not rely on volatile compounds, is required.

Camphene undergoes typical ionization and fragmentation patterns associated with monoterpenes [100] (Table 2). The peaks which represent the products from these reaction processes are detected (Figures 5 to 6). However, the proportion of the peaks corresponding to the ions are not equivalent to the findings of Wang, Španěl and Smith [100] thus, it cannot be safely concluded that these peaks represent camphene. A similar situation exists for bornyl acetate. Many of the ions expected to occur from the reactions of the chosen precursor ions with bornyl acetate are formed (Figures 5 to 6), yet the proportion of the ions produced do not represent those observed in previous studies [50]. Again, the detection of bornyl acetate cannot be confirmed. Of the reactions with valerenal, valerenic acid and 15-acetoxy valeranone, few potential ion products can be identified for H_3O^+ and one for NO^+ ion products. This does not provide sufficient evidence that the ion peaks seen stand for the ions formed from these compounds.

4.4.4. *Cannabis sativa* (industrial hemp)

Cannabis sativa volatiles are composed among others, of several fragrant monoterpenes [67, 68]. As reported in chapter 2 and by Wang, Španěl and Smith [100], analysis of monoterpenes, using SIFT-Ms is a difficult task. The detection and identification of the major monoterpenes in *Cannabis sativa* cannot be done by merely finding peaks which represent the product/fragment ions that are formed during reactions with H_3O^+ and NO^+ . Tables 7 and 8 illustrate the similarity in fragmentation patterns amongst monoterpenes. However the proportion in which these peaks occur are relevant and contribute to the identification of the compound being detected. The combination of

peak value (m/z) and proportion of peaks, with respect to other peaks, form a fingerprint for the compound. I selected the 7 most abundant volatiles reported in *Cannabis* [67, 68] and searched for evidence of the resulting ion m/z values.

4.4.4.1. *Cannabis sativa* H_3O^+ Reactions

For both, *Cannabis sativa* seeds and leaves, the protonated parent compound is the dominant reaction product between terpinolene and H_3O^+ while, H_2O elimination is the dominant reaction between 2-methyl-1-butanol and H_3O^+ [86, 100]. Therefore, peaks at m/z 137 (Fig.7b; Fig.9b) and m/z 71 (Fig. 7a; ion peak not shown in Fig. 9a) could potentially represent terpinolene and 3-methyl-2-butanol, respectively. Since these molecules only have one significant reaction product, it is difficult to conclude that these peaks are true representations of terpinolene and 3-methyl-1-butanol and further analysis is required, that is, NO^+ reactions. The protonated parent compound (m/z 137) is a major ion produced for several monoterpenes and cannot be used as an indicator of terpinolene specifically. Similarly, a single ion (m/z 71) cannot be used to authenticate 3-methyl-1-butanol and further analysis is required.

Myrcene, ocimene, β -pinene and limonene all have similar reaction processes with H_3O^+ [100]. The proportion of the products from these reaction processes are used to determine if the molecule is represented in the spectra. Although characteristic peaks/ion masses are present in the spectra for these monoterpenes, the proportion of the peaks do not resemble those of the monoterpenes of interest (myrcene, ocimene, β -pinene and limonene) for *Cannabis sativa* leaf analysis. As shown in Chapter 2 and Wang, Španěl and Smith [100], these peaks could aid in identifying the total monoterpene content present in the sample, but not individual spectral compounds.

Several ions are shown to be produced as a result of the reactions from H_3O^+ with linalool [4]. Two ions, C_6H_9^+ and $\text{C}_{10}\text{H}_{17}^+$, comprise majority of the total ions formed from the above mentioned reaction and are used as indicators of linalool [4]. Again, peaks representing these ions, m/z 81 (47912 cps, Fig. 7a; 6106 cps, Fig. 9a) and m/z 137 (3222 cps, Fig.7b; 8823 cps, Fig.9b), are present in the spectra for linalool, but the proportion of the peaks do not resemble those described by Amelynck, Schoon, Kuppens, Bultinck and Arijs [4]. Thus, it cannot be assumed that linalool has been detected in the *Cannabis sativa* samples.

In contrast to *Cannabis sativa* leaf analysis, *Cannabis sativa* seed analysis shows that myrcene, ocimene and limonene have a similar proportion of ions to those previously reported [100], with respect to the major and minor ions formed, while β -pinene has an essentially equivalent ion ratio reported by Wang, Španěl and Smith [100]. Based on this information, I would conclude that β -pinene has been detected by the instrument, although, the detection of the other monoterpenes cannot be excluded. Further analysis with NO^+ analysis would help strengthen this interpretation.

4.4.4.2. *Cannabis sativa* NO^+ Reactions

Although charge transfer is not a common reaction for alcohol- NO^+ reactions, it is interesting that a significant peak which represents this ion (m/z 88) (3535 cps, Fig. 10a) was found in great abundance in the SIFT-MS analysis of *Cannabis sativa* where we know 3-methyl-1-butanol is a major constituent. The other fragment ions for this compound (m/z 81 and 71) (Fig. 8a; Fig. 10a) are detected as minor peaks and cannot be used to confirm the identification of 3-methyl-1-butanol in these samples.

Most monoterpene- NO^+ reactions have similar reaction processes [100], so the

proportions of the products formed from these reactions are used to determine if the molecule is represented in the spectra. The two ions formed from the reaction of terpinolene and NO^+ (m/z 121 and m/z 136) do not appear in the same proportion as found for the standard compound in chapter 2. The m/z 121 ion is an expected fragment ion (Table 4). However, ion peaks for *Cannabis sativa* leaf and seed spectra are not visible at m/z 121 due to low cps (0.3% and 0.6% of total respectively) and therefore cannot be used as an indicator for terpinolene detection. On the other hand, a similar proportion of product ions for ocimene (leaf analysis) (25% m/z 92, 25% m/z 93 and 50% m/z 136) and myrcene (seed analysis) (16% m/z 92, 44% m/z 93 and 40% m/z 136) were seen when compared to previously published data for these compounds (29%, 22%, 49% and 11%, 44%, 45%, respectively) [100]. This may suggest that ocimene and myrcene were detected by SIFT-MS analysis of *Cannabis sativa* leaves and seeds respectively, when reacted with NO^+ .

Similar to the H_3O^+ reactions, two ions (m/z 96 and m/z 136) make up the bulk of total ion percent for linalool [4]. SIFT-MS spectra analysis of *Cannabis sativa* leaves and seeds show a peak to be present at m/z 136 and m/z 96, however, the ion count at m/z 96 is minimal (30 cps, Fig. 8a; 88 cps, Fig. 10a) and does not conform to previously reported data [4]. As a result, the detection and identification of linalool in the *Cannabis sativa* samples cannot be confirmed.

4.5. Conclusions and Future Applications

SIFT-MS provides an alternative method for the determination of compounds found in plant material. This method was not successful to detect valeric acid, heptanoic acid, octanoic acid, nonanoic acid, salicylic acid or *o*-cresol in *Polygala senega*. SIFT-

MS has detected with a reasonable level of confidence hexanoic acid and methyl salicylate in *Polygala senega* using H_3O^+ . However, I was unable to confirm the presence of the abovementioned compounds using NO^+ . As for the *Cannabis sativa* leaf and seed samples, terpinolene and 3-methyl-1-butanol did not readily conform to the standards' spectral data and therefore are not detected with confidence. Spectral data strongly suggests that ocimene is present in leaf samples and β -pinene and myrcene are present in seed samples. The other monoterpenes cannot be included or excluded with certainty due to the fact that majority of the characteristic ion peaks are present in the spectra.

For the task of natural product research, in other words, the detection and identification of VOCs emitted from biological samples, special considerations are required. The sensitivity of the instrument allows the successful detection of volatile compounds, however, often producing complex mass spectra. Plant samples bring another level of difficulty to this type of analysis, being in essence a complex mixture. Fragment ions formed from the reactions of the volatiles with the precursor ions may react with each other to form various unexpected adduct ions. Of the hundreds of constituents plants are composed of, few are in high abundance while, the majority, although essential to the medicinal or aromatic characteristics of the plant, remain in low or trace amounts. The constituents which account for the bulk of the compounds may overwhelm the instrument by comprising majority of the compounds present in the flow tube during analysis. The precursor ions react primarily with these compounds and create the illusion that few significant volatiles are present when reviewing the spectra; however, ion peaks with low counts may represent significant ions. Diluting the plant

sample may overcome this issue. A data library is an essential tool which aids the identification of unknown compounds from such spectra. When seeking to locate a compound of medicinal or commercial value from a plant sample, the fingerprint, or fragmentation pattern of the compound should be known. This valuable information may be obtained by analysing a pure sample of the compound being sought after using the SIFT-MS. Further studies continuing the development of an extensive SIFT-MS standard data library would relieve some of the difficulties associated with SIFT-MS and natural product analysis. Also, the optimization of a method to investigate large molecular weight compounds with the accompaniment of classical methods such as GC-MS to corroborate results would improve analyses. By understanding the operation of the instrument, having basic knowledge about the valuable compounds being sought and having the means to confirm uncertain data with alternative methods, SIFT-MS can aid in the detection and identification of volatile compounds from natural products. Thus, the strength of SIFT-MS analysis does not lie in the detection of NCEs, but in the search for known and relatively abundant compounds of value in biological samples.

It appears that in the current state of this technology, SIFT-MS could be applied to specific major compounds producing characteristic mass spectra. Focusing on one or two compounds per plant, quantitative SIFT-MS analyses may need to be developed and linked to applied problems such as phenological and quality assurance programs in production systems. Possible future applications using the SIFT-MS may include analyses of various economically valuable plant species and their components. If we can qualitatively identify and quantify known compounds of interest, then we can examine how seasonal developmental changes affect the quantity of the compound in the sample

and determine when the plant should be harvested.

The ultimate development of a portable instrument to analyze biological samples containing specific compounds of interest may increase agronomic productivity. The field operable instrument would eliminate lengthy preparatory procedures. Furthermore, specific compounds may be detected without the need to damage the plant tissue. Our results provide a foundation for future investigations of the utility of SIFT-MS for plant VOC analysis and commercial applications.

4.6. Acknowledgments

I thank Dr. Tarlok Sahota of the Thunder Bay Agricultural Research Station (TBARS) for providing the *Cannabis sativa* (industrial hemp) samples used in this study.

CHAPTER 5.0. REFERENCES

1. Abel, U., C. Koch, M. Speitling and F. G. Hansske (2002). "Modern methods to produce natural-product libraries." Current Opinion in Biotechnology **6**(453-458): 453.
2. Aburjai, T. and F. M. Natsheh (2003). "Plants Used in Cosmetics." Phytotherapy Research **17**: 987-1000.
3. Adams, N. G. and D. Smith (1976). "The Selected Ion Flow Tube (SIFT); A Technique For Studying Ion-Neutral Reactions." International Journal of Mass Spectrometry and Ion Physics **21**: 349-359.
4. Amelynck, C., N. Schoon, T. Kuppens, P. Bultinck and E. Arijs (2005). "A selected ion flow tube study of the reactions of H_3O^+ , NO^+ and O_2^{*+} with some oxygenated biogenic volatile organic compounds." International Journal of Mass Spectrometry **247**: 1-9.
5. Amigo, J. M., T. Skov, R. Bro, J. Coello and S. Maspoch (2008). "Solving GC-MS Problems with PAPFAC2 " TrAc Trends in Analytical Chemistry **27**(8): 714-725.
6. Armstrong, J. W. (1999). "A review of high-throughput screening approaches for drug discovery." Combinatorial Chemistry Review 26-28.
7. Balunas, M. J. and D. Kinghorn (2005). "Drug discovery from medicinal plants." Life Sciences **78**: 431-441.
8. Bentley, K. W. (1959). Mono- and Sesquiterpenoids. The Chemistry of Natural Products. P. de Mayo. Vol. 2. New York, Interscience Publishers, Inc.
9. Bohme, D. K. (1975). "The Kinetics of Proton Transfer" Interactions Between Ions and Molecules. Ed. P. Ausloos. New York, Plenum Press: 489-504.
10. Briggs, C. J. (1988). "Senega snakeroot: a traditional Canadian herbal medicine." Canadian Pharmaceutical Journal **121**: 199-201.
11. Bromm, B., E. Scharein, U. Darsow and J. Ring (1995). "Effects of menthol and cold on histamine-induced itch and skin reactions in man." Neuroscience Letters **187**: 157-160.
12. Buck, L. and R. Axel (1991). "A novel multigene family may encode odorant receptors: a molecular basis for odor recognition." Cell **65**: 175-187.

13. Butler, M. S. (2004). "The Role of Natural Product Chemistry in Drug Discovery." Journal of Natural Products **67**: 2141-2153.
14. Butzke, C. E., T. J. Evans, S. E. Ebeler (1998). Detection of Cork Taint in Wine Automated solid Phase Microextraction in Combination with GC/MS-SIM. Chemistry of Wine Flavor. A. L. Waterhouse and S. E. Ebeler. New York, Oxford University Press.
15. Callaway, J. C. (2004). "Hemp seed as a nutritional resource: An overview." Euphytica **140**: 65-72.
16. Cappiello, A. (2007). Advances in LC-MS instrumentation. Amsterdam, Boston, Elsevier.
17. Carroll, W., W. Lenney, T. Wang, P. Španěl, A. Alcock and D. Smith (2005). "Detection of Volatile Compounds Emitted by *Pseudomonas aeruginosa* Using Selected Ion Flow Tube Mass Spectrometry." Pediatric Pulmonology **39**: 452-456.
18. Chopra, I. C. and R. N. Chopra (1957). "The use of Cannabis drugs in India." Bulletin on Narcotics (1): 4-29.
19. Circosta, C., R. De Pasquale, S. Samperi, A. Pino and F. Occhiuto (2007). "Biological and analytical characterization of two extracts from *Valeriana officinalis*." Journal of Ethnopharmacology **112**: 361-367.
20. Clardy, J. and C. Walsh (2004). "Lessons from natural molecules." Nature **432**: 829-837.
21. Cragg, M. G., D. J. Newman and K. M. Snader (1997). "Natural Products in Drug Discovery and Development." Journal of Natural Products **60**(1): 52-60.
22. Demyttenaere, J. and S. van Ruth (2001). "Natural flavours. Overviews and applications of analytical methods and microbial production." Biomolecular Engineering **17**: 119.
23. Drews, J. (2000). "Drug Discovery: A Historical Perspective." Science **287**(5460): 1969-1964.
24. Ebadi, M. (2002). Pharmacodynamic Basis of herbal Medicine. Boca Raton, CRC Press.
25. Estrada, A., G. Katselis, B. Laarveld and B. Barl (2000). "Isolation and evaluation of immunological adjuvant activities of saponins from *Polygala senega* L." Comparative Immunology, Microbiology and Infectious Diseases **23**: 27-43.

26. Ferenczy, L., L. Gracza and I. Jacobey (1958). "An antibacterial preparation from Hemp (*Cannabis sativa* L.)." Naturwissenschaften **45**: 188.
27. Fuller, G. H., R. Steltenkamp and G. A. Tisserand (1964). The Gas Chromatograph with Human Sensor: Perfume Annals of the New York Academy of Sciences. **116**: 711-724.
28. Gao, X. Q. and L. Bjork (2000). "Valerenic acid derivatives and valepotriates among individuals, varieties and species of *Valeriana*." Fitoterapia **71**: 19-24.
29. Garcia, I., M. C. Ortiz and J. M. Aldama (2004). "Three-way models and detection capability of a gas chromatography-mass spectrometry method for the determination of clenbuterol in several biological matrices: the 2002/657/EC European Decision." Analytica Chimica Acta **515**(1): 55-63.
30. Gillies, B., H. Yamazaki and D. W. Armstrong (1987). "Production of Flavor Esters by Immobilized Lipase." Biotechnology Letters **9**(10): 709-714.
31. Grosch, W. (2001). "Evaluation of key odorants of foods by dilution experiments, aroma models and omission." Chemical Senses **26**: 533-545.
32. Guenther, E. (1952). The Essential Oils. Individual Essential Oils Of The Plant Families *Ericaceae*, *Betulaceae*, *Valerianaceae*, *Verbenaceae*, *Cistaceae*, *Cruciferae*, *Liliaceae*, *Iridaceae*, *Araceae*, *Palmae*, *Cyperaceae*, *Moraceae*, *Aristolochiaceae*, *Chenopodiaceae*, *Ranunculaceae*, *Euphorbiaceae*, *Malvaceae*, *Usneaceae*, *Podocarpaceae*, *Pinaceae*, *Taxodiaceae*, and *Cupressaceae*. New York, D. Van Nostrand Company, Inc. **6**: 23-34.
33. Guth, H. and W. Grosch (1999). Important odorants in foods by dilution techniques. Flavor Chemistry. R. Teranishi, E. L. Wick and I. Hornstein. New York, Kluwer Academic/Plenum: 377-386.
34. Haag, J. D., M. J. Lindstrom and M. N. Gould (1992). "Limonene-induced Regression of Mammary Carcinoma." Cancer Research **52**: 4021-4026.
35. Hadley, S. and J. J. Petry (2003). "Valerian." Complementary and Alternative Medicine **67**(8): 1755-1758.
36. Hanson, J. R. (1972). Introduction. Chemistry of Terpenes and Terpenoids. N. A. A. London, Academic Press: 1-6.
37. Hargis, L. G. (1988). Analytical Chemistry, Principles and Techniques. New Jersey, Prentice-Hall, Inc.

38. Hayashi, S. and H. Kameoka (1995). "Volatile Compounds of *Polygala senega* L. variation *latifolia* Torrey et Gray Roots." Flavour and Fragrance Journal **10**: 273-280.
39. Hoffman, D. (1996). The Complete Illustrated Holistic Herbal. Rockport, MA, Element Books Inc.
40. Horning, E. C., D. I. Carroll, I. Dzidic, K. D. Haegele, S-N. Lin, C. U. Oertill and R. N. Stillwell (1977). "Development and use of analytical systems based on mass spectrometry." Clinical Chemistry **23**(1): 13-21.
41. Houghton, P. J. (1988). "The biological activity of valerian and related plants." Journal of Ethnopharmacology **22**: 121-142.
42. <http://www.kranalytical.co.uk/SIFTMS.html>. (2008). "KR Analytical." 2008.
43. Hwang, Y-S., K-H. Wu, J. Kumamoto, H. Axelrod and M. S. Mulla (1985). "Isolation and identification of mosquito repellants in *Artemisia vulgaris*." Journal of Chemical Ecology **11**(9): 1297-1306.
44. Jalees, S., S. K. Sharma, S. J. Rahman and T. Verghese (1993). "Evaluation of insecticidal properties of an indigenous plant, *Cannabis sativa* Linn., against mosquito larvae under laboratory conditions." Journal of Entomological Research **17**(2): 117-120.
45. Joulien, S. (1849). "Substance anesthesique employee en chine dans le commencement du IIIeme siecle de notre ere pour paralyser momentanement la sensibilite." Comptes rendus hebdomadaires des séances de l'Académie des sciences, **28**: 195.
46. Katselis, G. S., A. Estrada, D. K. J. Gorecki, Dennis and B. Barl (2007). "Adjuvant activities of saponins from the root of *Polygala senega* L." Canadian Journal of Physiology and Pharmacology **85**: 1184-1194.
47. Klich, R. (1975). "Behavior disorders in childhood and their therapy." Die Medizinische Welt **26**: 1251-1254.
48. Koroch, A. R., H. R. Juliani and J. A. Zygadio (2007). Bioactivity of essential oils and their components. Flavors and Fragrances. R. G. Berger. Berlin, Springer.
49. Kubista, J., P. Španěl, K. Dryahina, C. Workman and D. Smith (2006). "Combined use of gas chromatography and selected ion flow tube mass spectrometry for absolute trace gas quantification." Rapid Communications In Mass Spectrometry **20**: 563-567.

50. Letchamo, W., W. Ward, B. Heard and D. Heard (2004). "Essential Oil of *Valeriana officinalis* L. Cultivars and Their Antimicrobial Activity As Influenced by Harvesting Time under Commercial Organic Cultivation." Journal of agricultural and food chemistry **52**: 3915-3919.
51. Leung, A. Y. (1980). Encyclopedia of common natural ingredients used in food, drugs and cosmetics. New York, New York, John Wiley and Sons Inc.
52. Lias, S.G. in: Mallard, W.G. and P.J. Linstrom, eds. *Ionization Energy Evaluation in NIST Chemistry WebBook, NIST Standard Reference Database Number 69*. 2000, National Institute of Standards and Technology: Gaithersburg, MD.
53. Lide, D. R. (2006). CRC Handbook of Chemistry and Physics. Boca Raton, Florida, Taylor and Francis Group, LLC.
54. Lis-Balchin, M. (1997). "Essential oils and aromatherapy: their modern role in healing." The journal of the Royal Society for the Promotion of Health **117**(5): 324-329.
55. Ma, T. S. (1969). Analysis of Carboxylic Acids. The Chemistry of Carboxylic Acids and Esters. S. Patai. London, New York, Interscience Publishers.
56. Mahdi, J. G., A. J. Mahdi, A. J. Mahdi and I. D. Bowen (2006). "The historical analysis of aspirin discovery, its relation to the willow tree and antiproliferative and anticancer potential." Cell proliferation **39**: 147-155.
57. McClellan, A. L. (1963). Tables of Experimental Dipole Moments. San Francisco, W. H. Freeman and Company.
58. Mechoulam, R. and Y. Gaoni (1967). "Recent Advances in the Chemistry of Hashish." Progress in the chemistry of organic natural products **25**: 175-213.
59. Newman, D. J., G. M. Cragg and K. M. Snader (2003). "Natural Products as Sources of New Drugs over the Period 1981–2002." Journal of Natural Products **66**(7): 1022-1037.
60. Pavlou, A. K. and A. P. F. Turner (2000). "Sniffing out the Truth: Clinical Diagnosis Using the Electronic Nose." Clinical Chemistry and Laboratory Medicine **38**(2): 99-112.
61. Peirce, A. (1999). The American Pharmaceutical Association Practical Guide to Natural Medicines. New York, William Morrow and Company Inc.
62. Penault, C., P. Španěl and D. Smith (2005). Detection of *H. Pylori* infection by breath ammonia following urea ingestion. Breath Analysis for Clinical Diagnosis and Therapeutic Monitoring. Singapore, Works Scientific: 393-399.

63. Perez-Cacho, P. R. and R. L. Rouseff (2008). "Fresh Squeezed Orange Juice Odor: A Review." Critical Reviews in Food Science and Nutrition **48**: 681-695.
64. Peterson, E. A. and E. Overman Larry (2004). "Contiguous stereogenic quaternary carbons: A daunting challenge in natural products synthesis." PNAS **101**(33): 11943-11948.
65. Pezzuto, J. M. (1997). "Plant derived anti-cancer agents." Biochemical Pharmacology **53**: 121-133.
66. Pringle, H. (1997). "Ice age community may be earliest known net hunters." Science **277**: 1203-1204.
67. Ross, S., A. and M. ElSohly, A. (1996). "The Volatile Oil Composition of Fresh and Air-dried Buds of *Cannabis sativa*." Journal of Natural Products **59**: 49-51.
68. Rothschild, M., G. Bergstrom and S. Wangberg (2005). "*Cannabis sativa*: volatile compounds from pollen and entire male and female plants of two variants, Northern Lights and Hawaiian Indica." Botanical Journal of the Linnaean Society **147**: 387-397.
69. Safaralie, A., S. Fatemi and F. Sefidkon (2008). "Essential oil composition of *Valeriana officinalis* L. roots cultivated in Iran comparative analysis between supercritical CO₂ extraction and hydrodistillation." Journal of Chromatography A **1180**: 159-164.
70. Sarker, S. D. and L. Nahar (2007). Chemistry for Pharmaceutical Students General, Organic and Natural Product Chemistry. Chichester, John Wiley and Sons.
71. Savenhed, R., H. Boren and A. Grimvall (1985). "Stripping analysis and chromatographic sniffing for the source identification of odorous compounds in drinking water." Journal of Chromatography A **328**: 219-231.
72. Schwab, W., R. Davidovich-Rikanati and E. Lewinsohn (2008). "Biosynthesis of plant derived flavor compounds." The Plant Journal **54**: 712-732.
73. Shaw, P. E. (1991). Fruits II. Volatile compounds in foods and beverages. H. Maarse. New York, Marcel Dekker, Inc.: 305-327.
74. Sidgwick, N. V., G. C. Hampson and R. J. B. Marsden (1934). A Table of Dipole Moments. London, Gurney and Jackson.
75. Smith, D. and N. G. Adams (1987). "The Selected Ion Flow Tube (Sift): Studies of Ion-Neutral Reactions " Advances in Atomic and Molecular Physics **24**: 1-49.

76. Smith, D., A. M. Diskin, Y. Ji and P. Španěl (2001). "Concurrent use of H_3O^+ , NO^+ and O_2^+ precursor ions for the detection and quantification of diverse trace gases in the presence of air and breath by selected ion-flow tube mass spectrometry." International Journal of Mass Spectrometry **209**: 81-97.
77. Smith, D. and P. Španěl (1996). "Review The novel SIFT approach to trace gas analysis of air and breath " Rapid Communications In Mass Spectrometry **10**: 1183-1198.
78. Smith, D. and P. Španěl (2005). "Selected Ion Flow Tube Mass Spectrometry (SIFT-MS) For On-Line Trace Gas Analysis." Mass Spectrometry Reviews **24**: 661-700.
79. Souleyre, E. J. F., D. R. Greenwood, E. N. Friel and S. Karunairetnam (2005). "An alcohol acyl transferase from apple (cv. Royal Gala), MpAAT1, produces esters involved in apple fruit flavor." FEBS **272**: 3132-3144.
80. Španěl, P., A. M. Diskin, S. M. Abbot, T. Wang and D. Smith (2002). "Quantification of volatile compounds in the headspace analysis of aqueous liquids using selected ion flow tube mass spectrometry." Rapid Communications In Mass Spectrometry **16**: 2148-2153.
81. Španěl, P., M. Pavlik and D. Smith (1995). "Reactions of H_3O^+ and OH^- ion with some organic molecules; applications to trace gas analysis in air." International Journal of Mass Spectrometry and Ion Processes **145**: 177-186.
82. Španěl, P., D. Smith (1996). "A selected on flow tube study of the reactions of NO^+ and O_2^+ ions with some organic molecules: The potential for trace gas analysis of air." Journal of Chemical Physics **104**(5): 1893-1899.
83. Španěl, P., P. Rolfe, B. Rajan and D. Smith (1996). "The Selected Ion Flow Tube (SIFT)- A Novel Technique for Biological Monitoring" The Annals of Occupational Hygiene **40**(6): 615-626.
84. Španěl, P. and D. Smith (1996). "Selected ion flow tube: a technique for quantitative trace gas analysis of air and breath." Medical & Biological Engineering & Computing **34**: 409-419.
85. Španěl, P., Y. Ji and D. Smith (1997). "SIFT-MS studies of the reactions of H_3O^+ , NO^+ and O_2^+ with a series of aldehydes and ketones." International Journal of Mass Spectrometry and Ion Processes **165/166**: 25-37.
86. Španěl, P. and D. Smith (1997). "SIFT studies of the reactions of H_3O^+ , NO^+ and O_2^+ with a series of alcohols." International Journal of Mass Spectrometry and Ion Processes **167/168**: 375-388.

87. Španěl, P. and D. Smith (1998). "SIFT studies of the reactions of H_3O^+ , NO^+ and O_2^+ with a series of volatile carboxylic acids and esters." International Journal of Mass Spectrometry and Ion Processes **172**: 137-147.
88. Španěl, P. and D. Smith (1998). "SIFT studies of the reactions of H_3O^+ , NO^+ and O_2^+ with several ethers " International Journal of Mass Spectrometry and Ion Processes **172**: 239-247.
89. Španěl, P. and D. Smith (1999). "Selected Ion Flow Tube - Mass Spectrometry: Detection and Real-time Monitoring of Flavours Released by Food Products." Rapid Communications In Mass Spectrometry **13**: 585-596.
90. Španěl, P. and D. Smith (2007). "Selected ion flow tube mass spectrometry for on-line gas analysis in biology and medicine." European Journal of Mass Spectrometry **13**: 77-82.
91. Stark, R. (1981). Guide to Indian Herbs. Vancouver, Hancock House Publishers Inc.
92. Su, T. and W. J. Chesnavich (1982). "Parameterization of the ion-polar molecule collision rate constant by trajectory calculations." Journal of Chemical Physics **76**: 5183-5185.
93. Taura, F., S. Morimoto and Y. Shoyama (1996). "Purification and Characterization of Cannabidiolic-acid Synthase from Cannabis sativa L.. Biochemical Analysis Of A Novel Enzyme That Catalyzes The Oxidocyclization Of Cannabigerolic Acid To Cannabidiolic Acid." Journal of Biological Chemistry **271**: 17411-17416.
94. Taylor, A. J. and R. S. T. Linforth (1996). "Flavour release in the mouth." Trends in Food Science **7**: 444-448.
95. Thaler, E. R., D. W. Kennedy and W. C. Hanson (2001). "Medical Applications of Electronic Nose Technology: Review of Current Status." American Journal of Rhinology **15**(5): 291-295.
96. Turcotte, C. and N. Kenkel (1997). The Ethnobotany and Economics of Seneca Snakeroot (*Polygala senega* L.). Issues in the North. J. Oakes and R. Riewe, University of Manitoba. **2**.
97. Ulrich, D., E. Hoberg, A. Rapp and S. Kecke (1997). "Analysis of strawberry flavour-discrimination of aroma types by quantification of volatile compounds." Zeitschrift für Lebensmittel-Untersuchung und-Forschung Q **205**: 218-223.
98. Van Klingerren, B. and M. Ten Ham (1976). "Antibacterial activity of delta9-tetrahydrocannabinol and cannabidiol." Antonie Van Leeuwenhoek **42**(1-2): 9-12.

99. van Ruth, S. M. (2001). "Methods for gas chromatography-olfactometry: a review." Biomolecular Engineering **17**: 121-128.
100. Wang, T., P. Španěl and D. Smith (2003). "Selected ion flow tube, SIFT, studies of the reactions of H_3O^+ , NO^+ and O_2^+ with eleven $\text{C}_{10}\text{H}_{16}$ monoterpenes." International Journal of Mass Spectrometry **228**: 117-126.
101. Wang, T., P. Španěl and D. Smith. (2004). "A selected ion flow tube study of the reactions of H_3O^+ , NO^+ and O_2^{++} with some phenols, phenyl alcohols and cyclic carbonyl compounds in support of SIFT-MS and PTR-MS." International Journal of Mass Spectrometry **239**:139-146.
102. Wasim, K., I-U. Haq and A. Mohammad (1995). "Antimicrobial studies of the leaf of *Cannabis sativa* L." Pakistan Journal of Pharmaceutical Sciences **8**(1): 29-38.
103. Whittaker, D. (1972). The Monoterpenes. Chemistry of Terpenes and Terpenoids. A. A. Newmann. London, Academic Press: 11-82.
104. Williamson, E. M. (2001). "Synergy and other interactions in phytomedicine." Phytomedicine **8**: 401-409.
105. Williamson, E. M. and F. J. Evans (2000). "Cannabinoids in clinical practice." Drugs **60**: 1303-1314.
106. Younes, R. N., A. D. Varella and I. B. Suffredin (2007). "Discovery of new antitumoral and antibacterial drugs from Brazilian plant extracts using high throughput screening." Clinics **62**(6): 763-768.
107. Young, H., J. M. Gilbert, S. H. Murray and R. D. Ball (1996). "Casual Effects of Aroma Compounds on Royal Gala Apple Flavours." Journal of the Science of Food and Agriculture **71**: 329-336.
108. Zhang, J., T. D. Y. Chung and K. R. Oldenburg (1999). "A Simple Statistical Parameter for Use in Evaluation and Validation of High Throughput Screening Assays." Journal of Biomolecular Screening **4**(2): 67-73.